Automation in Dynamic Analysis and Generative Design of Prestressed Concrete Railway Bridge Infrastructures

Khuong Le Nguyen[1], Thong M. Pham[3], Khanh Nguyen[4], Saeed Banihashemi[5*]

[1] Department of Civil Engineering, University of Transport Technology, Hanoi, 100000, Vietnam; khuongln@utt.edu.vn

[2] Faculty of Arts and Design, University of Canberra, 11 Kirinari St, Bruce ACT 2617 khuong.lenguyen@canberra.edu.au

[3]UniSA STEM, University of South Australia, Mawson Lakes, SA 5095, Australia Email: thong.pham@unisa.edu.au

[4]Escuela Técnica Superior de Ingeniería Aeronáutica y del Espacio, Universidad Politécnica de Madrid, 3 Pza. Cardenal Cisneros, Madrid, 28040, Spain, khanhnguyen.gia@upm.es

[5]School of Built Environment, University of Technology Sydney, Australia. Saeed.Banihashemi@uts.edu.au

*Corresponding author

Abstract

This study presents an innovative method for the dynamic analysis and generative design of high-speed ballasted railway bridges subjected to High-Speed Locomotive Multiple Articulated (HSLM-A) train loads. Compliant with Eurocode standards, a comprehensive database of over 4 million data points was generated, including maximum vertical displacement and acceleration data for more than 10,000 bridges affected by ten HSLM-A models at speeds ranging from 150 to 350 km/h. The key contribution of this research lies in a novel surrogate model that incorporates semantic search and advanced decoding techniques, significantly enhancing the calculation time and accuracy of dynamic behaviour predictions for single-span high-speed railway bridges. The performance of the developed model was verified through case studies on existing 30m and 50m span bridges, evidenced by an R^2 value of 0.999, highlighting the model's precision and rapid prediction capabilities. Additionally, the research introduces a cutting-edge framework for optimising the cross-sectional geometry of prestressed concrete railway bridges. A case study was then conducted for a typical box girder bridge to identify 25 feasible solutions better than the original design in terms of mass per unit length. This research showcases the synergy between advanced technology and structural optimisation, and it opens new avenues for future studies in this field.

Keywords: Semantic Surrogate Modelling; High-Speed Railway Bridge Dynamics; Generative Design Optimisation; Structural Performance Prediction; Advanced Decoding Techniques.

1 Introduction

High-speed railway (HSR) systems represent a notable advancement in transportation, providing fast, environmentally friendly, and efficient travel options. The increasing global deployment of these systems has made the design and operation of high-speed railway bridges extremely important. Unlike slower, heavier freight trains that primarily induce quasi-static effects, high-speed passenger trains can potentially cause resonance when the frequency of the loading, determined by the train speed and axle spacing, approaches the natural frequency of the bridge. As new train designs with varying axle configurations are introduced and operate at increasingly high speeds, the likelihood of matching these frequencies increases. The complexity of these dynamic interactions, coupled with the need to design for future train developments, makes the analysis and design of high-speed railway bridges particularly challenging [1–5].

In addressing these challenges, simply supported prestressed concrete box girders have risen as a favourite structural solution. Renowned for their structural efficiency, these girders effectively resist dynamic forces and vibrations of high-speed train transit, offering great torsional stiffness and strength vital for maintaining bridge stability at high velocities [6–9]. Moreover, the incorporation of prestressing techniques significantly mitigates tension, enabling the construction of longer spans, thereby enhancing the durability and longevity of the structures [10–13].

Due to the many advantages of these structures, extensive research has delved into the dynamic performance of simple span railway bridge girders, using a multi-dimensional approach associated with various factors such as resonance, material properties, and friction [14–19]. More specifically, the authors [20–22] examined the resonance characteristics of bridges under high-speed train passage, revealing the critical need to differentiate between dominated train frequencies and bridge natural frequencies to mitigate resonance risks. They also demonstrated that axial stiffness between simple girders could significantly reduce vibrations near resonance conditions. Other researchers [23–27] focused on the interaction between the "train-bridge" system and bridge deck resonant vibrations, highlighting the importance of dynamic phenomena control at the wheel-rail contact level.

In the design process, modal analysis and time history analysis are often required to determine the dynamic behaviours such as displacements, accelerations, and bending moments of the bridge subjected to fast-moving train. Eurocode 1 [28] considers various high-speed load models (e.g., HSLM-A) for dynamic analyses of all railway bridges in the network. When new high-speed trains are designed with dynamic signatures that fall within the envelope of the HSLM-A models, additional dynamic checks of the bridges may not be required, as the bridges are already designed for this envelope of dynamic effects. However, for trains with characteristics outside this envelope, or as train technology evolves beyond the parameters considered in the original HSLM-A development, additional dynamic analysis may be necessary [29,30]. This approach ensures that bridges are prepared for future train designs, making the design process more efficient and the bridges safer and more reliable.

However, a critical challenge remains: incorporating dynamic analysis into a design framework,

especially different constraints and requirements are essential for comparing design alternatives [31,32]. To address this, various researchers have explored ways to optimise bridge designs for high-speed trains. For example, Cho *et al.* [33] proposed a method to determine the optimal span length of railway bridges, focusing on minimising dynamic responses to high-speed trains. Similarly, Song and Lee [34] advanced this field by introducing sophisticated techniques for assessing the interaction between bridges and high-speed vehicles. Futher, Zhai et al. [35] highlighted the progress in train-bridge interaction models and underscored the critical role of accurate track modeling. These studies collectively enhance our understanding of how to design bridges that can efficiently support high-speed rail systems while ensuring safety and longevity.

Despite these advances, opportunities remain for further innovation in bridge design optimization. While significant advances have been made through probabilistic approaches by Allahvirdizadeh *et al.* [36] and surrogate-assisted reliability-based design optimization [37], the integration of exhaustive dynamic analysis with cross-sectional optimization using semantic search and generative design techniques remains to be fully explored. In recent years, emerging paradigms such as large language models (LLMs) and neuro-symbolic models have demonstrated promising capabilities in related fields. For instance, Wong *et al.* [38] and Dikmen *et al.* [39] have shown that LLMs, when adapted with construction-specific knowledge, can enhance tasks like risk identification and damage detection in infrastructure projects. These advances offer valuable insights that could extend to the dynamic analysis and design optimization of prestressed concrete railway bridges. Similarly, Onchiş *et al.* [40] employed neuro-symbolic models for damage detection in structural components, providing a new direction for improving the reliability and explainability of computational models used in infrastructure maintenance. These studies, published in Computers in Industry, underscore the potential of combining data-driven techniques with traditional simulation-based methods to address complex design challenges.

To address these challenges, this research introduces an innovative approach combining a surrogate model with a generative design framework. The surrogate model accelerates the dynamic analysis by accurately predicting the performance of bridge designs without extensive simulations, while the generative design framework efficiently explores a broad spectrum of design alternatives to identify optimal cross-sectional configurations.

Key highlights of this research include:

- Comprehensive Database Development: Generating over 4 million data points covering displacement and acceleration data for more than 10,000 bridges, particularly focusing on High-Speed Locomotive Multiple Articulated (HSLM-A) trains.
- Surrogate Modelling for Efficient Analysis: The novel surrogate model, derived from this extensive database, significantly reduces the time required for dynamic analysis.
- Practical Application via KD-Railway Tool [41]: Integrating the surrogate model into the KD-Railway tool bridges the gap between research and application.
- Emphasis on Generative Design: This study adopts generative design in optimising the cross-

sectional design of bridges, utilising automation for enhanced design efficiency.

- Adherence to Standards: The design framework is aligned with Eurocode standards to increase its applicability in practice.

The findings of this research are summarised in a video presentation, which can be viewed in this Youtube video.

2 Methodology

2.1 Research Workflow Overview

The workflow on the dynamic analysis and generative design of prestressed concrete railway bridges is illustrated in Figure 1 and consists of four distinct stages:

Stage 1: Data Generation

The first stage involves generating the highest possible vertical acceleration and displacement data of 10,000 bridges subjected to loading of 10 HSLM-A train models. All bridges were designed in accordance with Eurocode 1 [28] and analysed using KD-Railway [41], an in-house software tool developed by the authors. Built on the open-source Cast3M finite element analysis solver [42] , KD-Railway specializes in dynamic analysis of railway bridges and automates several critical processes including moving load function generation and envelope diagram plotting. The tool's parallel computing capabilities and automated processes significantly enhance computational efficiency while maintaining accuracy comparable to commercial software, as validated through multiple case studies. Using this validated tool, a total of 4 million data points were generated.

Stage 2: Surrogate Model Development and Validation

Using the generated database, a surrogate model was developed to predict the envelope curves for the maximum acceleration and displacement of railway bridges under loading induced by HSLM-A train model. Subsequently, this surrogate model was employed to forecast the dynamic characteristics of two actual bridges that were in the initial set of 10,000 bridges of Stage 1. The predicted values were compared to those obtained using the Finite Element Method (FEM) in order to assess the reliability and accuracy of the model.

Stage 3: Generative Design Process

Based on the trained models, this step presented a design approach that generate an optimal cross-section design for simply-supported prestressed concrete box girder bridges while meeting multiple constraints and goals.

Stage 4: Case Study and Practical Implementation

The surrogate model was incorporated in a revised edition of the KD-Railway software and made available on GitHub. The proposed framework was utilised to produce 25 viable and optimal alternatives for the cross-section of a 30-m span simply-supported prestressed concrete box girder bridge. This phase

aimed to showcase the practicality of the surrogate model and the generative design process.

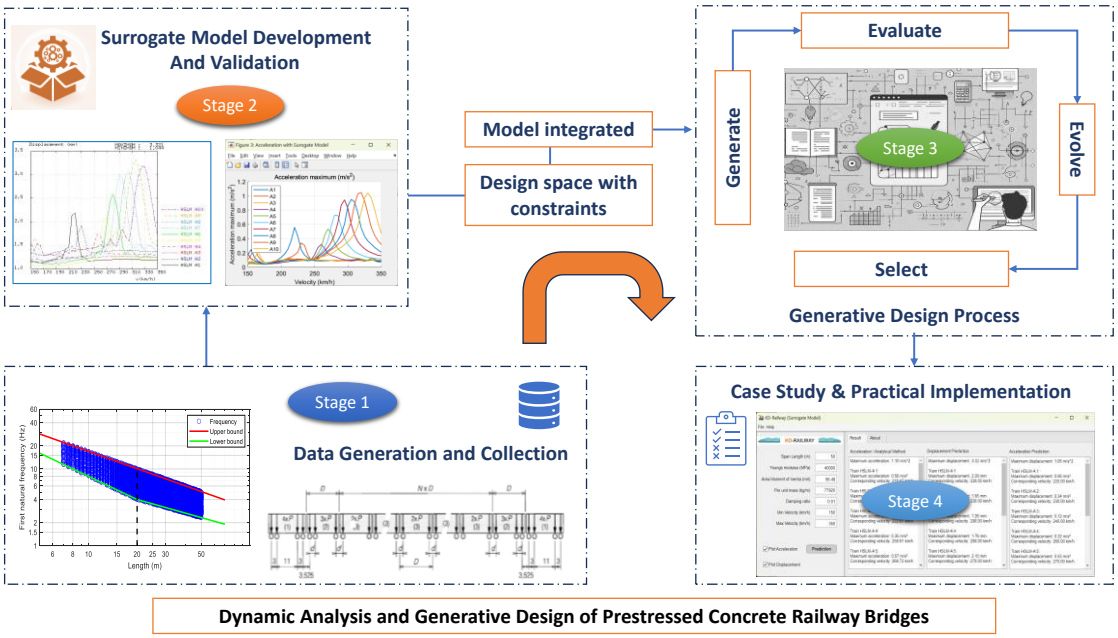

Figure 1. Research workflow

This study focuses exclusively on single-span simple supported beams without skew or complex geometry. This choice is deliberate and aligns with the prevalence of such structures in high-speed railway systems, as noted in the introduction. The methodology developed here is tailored for the preliminary design process, where simplicity and computational efficiency are paramount. While more complex bridge types exist, they typically require detailed design considerations beyond the scope of this preliminary design optimization framework.

2.2 Data Generation

2.2.1 Input parameters for dynamic analysis

The dynamic behaviour of high-speed ballasted railway bridges depends on several key factors, including the properties of the bridge's cross-section, span length, boundary conditions, material characteristics, and the moving load train models.

According to Eurocode 1 [28], the major input parameter for dynamic analysis is the initial natural frequency of the bridge. To improve the authenticity of the produced data, the frequency of each bridge was randomly generated within a range bounded by the upper and lower limits given in Eurocode 1. Furthermore, the bridge's mass, including its own weight and the weight of all its superstructural elements, is another crucial factor. The mass is quantified per unit length of the bridge and is determined following the guidelines provided by ERRI [43]. This assists engineers in determining suitable values for dynamic analyses.

Regarding train loads, Eurocode 1 [28] recommends a suite of standard load models that mimic the effects of various high-speed train types. Among these, the High-Speed Load Model (HSLM) is a key standard for representing the loads from articulated, conventional, and high-speed passenger trains. This

study focuses on bridges with simple support spanning from 7 to 50 meters. While this span range was used for database generation to ensure the surrogate model captures a wide spectrum of dynamic behaviors, it's important to note that the model's underlying parameters (mass, stiffness, frequency) are generic and not tied to any specific cross-sectional type.

The HSLM-A model has been consistently employed for all 10,000 bridges. The specific parameters for the HSLM load models are summarised in Table 1.

Table 1. Universal Train HSLM A1-A10 Parameters [28]

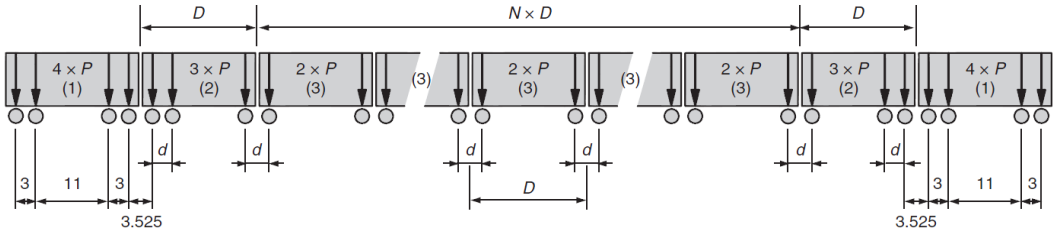

Universal train	Number of intermediate coaches N	Coach length D (m)	Bogie axle spacing d (m)	Point force P (kN)
A1	18	18	2.0	170
A2	17	19	3.5	200
A3	16	20	2.0	180
A4	15	21	3.0	190
A5	14	22	2.0	170
A6	13	23	2.0	180
A7	13	24	2.0	190
A8	12	25	2.5	190
A9	11	26	2.0	210
A10	11	27	2.0	210

Finally, the damping factor is another pivotal parameter within dynamic analysis. This study sets the damping factor at 1%, as commonly adopted for prestressed concrete railway bridges [43].

2.2.2 Frequency Considerations and HSLM-A Model Selection

In high-speed railway bridge dynamics, multiple frequency sources influence the structural response, including travelling frequencies from periodic axle loads, natural frequencies of the bridge and train, and frequencies arising from rail irregularities. Research by Fryba [44] and Yang et al. [45] has consistently demonstrated that the travelling frequency, determined by the spacing of train axles and bogies, is the most significant contributor to bridge dynamics. This finding is reflected in design standards such as Eurocode EN 1991-2:2003, which prioritizes travelling frequency in resonant speed calculations.

This study employs the HSLM-A model, which, while a simplification, effectively captures this crucial travelling frequency component. Although it does not account for train-bridge interaction or rail irregularities, studies by Majka and Hartnett [46] and Domenech et al. [47] have shown that rail irregularities, while significant for lateral dynamics and train response, have a comparatively minor influence on vertical bridge acceleration and dynamic amplification. The effects of rail irregularities are

indirectly addressed in Eurocode EN 1991-2:2003 through a coefficient φ″/2 in the dynamic amplification factor. However, recent research conducted by Patrick *et al.* [48] indicates that while this coefficient works well for displacement predictions, it may be less conservative for acceleration responses when using simplified moving load approaches rather than full train-track-bridge interaction models.

The HSLM-A model's focus on moving loads offers an optimal balance between accuracy and computational efficiency for vertical dynamics analysis. This approach aligns with current best practices in bridge engineering and is particularly suitable for the study's emphasis on vertical dynamic analysis and design optimization. While more detailed models would be necessary for studies on lateral dynamics, train safety, or passenger comfort, the HSLM-A model provides an appropriate level of detail for the purposes of this research.

2.2.3 Randomness selection of input parameters

The input parameters considered for this analysis include first natural frequency of the bridge (f_0), Young's modulus (E_k) in GPa, moment of inertia (I_k) in m^4, span length (L_k) in meters, and mass per unit length (m_k) in kg/m.

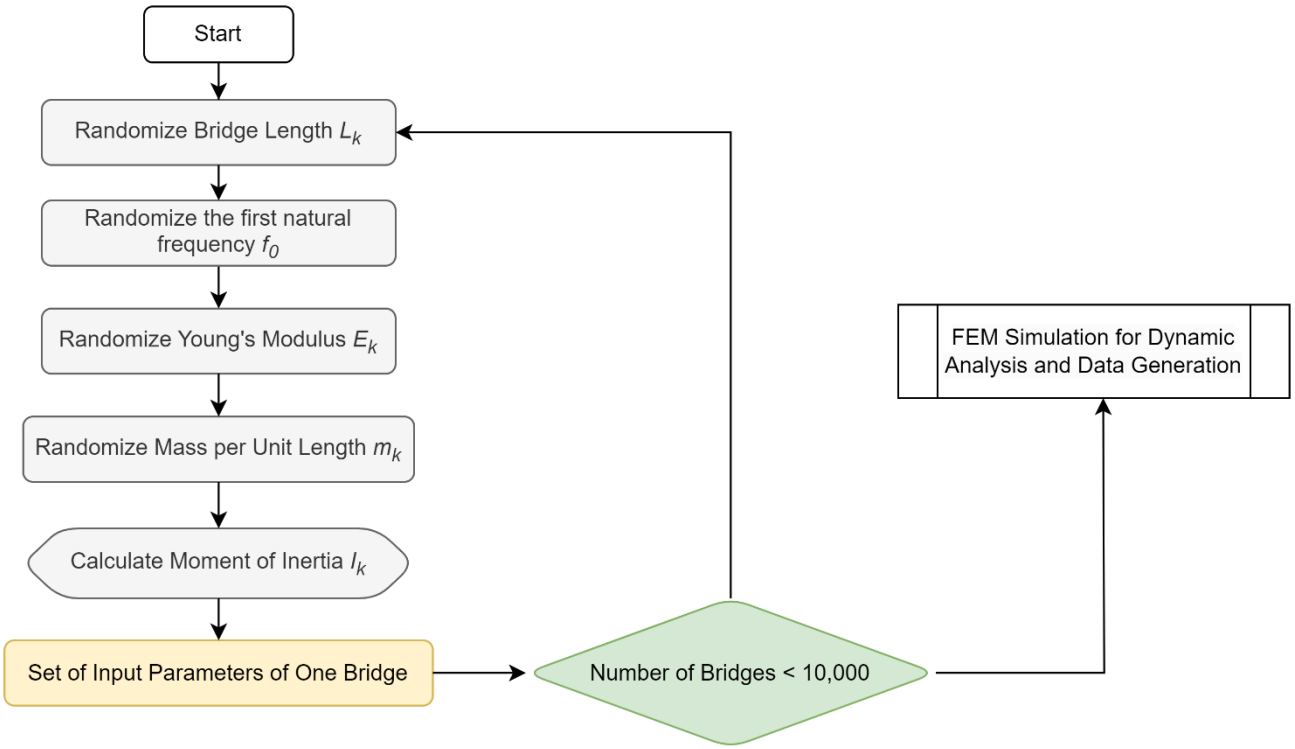

Figure 2. Flowchart of the Input and Output Generation Processes for 10,000 Railway Bridges

Figure 2 outlines the process for generating randomised data:

1. The length of the bridge (L_k) is randomised between [7, 50] meters using a uniform distribution.
2. Given L_k, the first natural frequency (f_0) was randomly generated within its bounds as per Eurocode 1.

3. Young's modulus (E_k) was randomised within the typical range for prestressed concrete, [30, 40] GPa.
4. The mass per unit length (m_k) was also randomised, considering the span length and corresponding guidelines to ensure a realistic distribution of bridge masses.
5. Finally, the moment of inertia (I_k) is calculated using the values obtained from the previous steps.

2.2.4 Data generated using KD-Railway source code

The data generation of 10,000 bridges was conducted through an automated process, leveraging the capabilities of the KD-Railway software [41]. To thoroughly analyse the characteristics of each bridge, a diverse range of train velocities ranging from 150 to 350 km/h, with increments of 5 km/h, was chosen. As a result, a total of 41 simulations was conducted for each train model. Therefore, to adhere to Eurocode rules, 10 distinct HSLM-A train models necessitates a substantial quantity of 410 simulations. A total of more than 4 million simulations were carried out, with each simulation yielding the maximum displacement and maximum acceleration of the respective bridge when subjected to a single train crossing at a specific speed.

The pivotal steps in the automated calculation process are outlined as follows (Figure 2):

1. Division into small groups: The bridges were batch-processed in smaller groups of 1,000 to improve computing performance. This method enabled parallel computations, resulting in a substantial optimisation of computational resource utilisation.
2. Initialization Loop: The computation sequence was designed with an initialisation loop, where each iteration corresponded to a bridge indexed from 1 to 10,000.
3. Bridge Construction and Load Application: In each iteration, the bridge model was constructed with the specified input parameters—length, elastic modulus, moment of inertia, and mass per unit length. The loadings were 10 different HSLM-A train models.
4. Result Recording: Upon completing the dynamic analysis for each bridge, the Cast3M software automatically compiled and recorded the results, including the maximum displacement and acceleration values as functions of train speed, were saved into individual .csv files for further processing and analysis.

The computation, conducted on a personal laptop with moderate specifications (All-in-One Desktop Computer, 11th Gen Intel Core i7-1165G7), spanned over four days. More than 4 million data points for maximum vertical acceleration and displacement were recorded. Figure 3 displays histograms for the input features: Young's modulus, moment of inertia, length, and mass per unit length, offering a visual representation of the distribution of these critical bridge parameters. The histograms demonstrate that the input parameters are distributed across their respective engineering-relevant ranges (e.g., Young's modulus from 30-40 GPa) with sufficient sampling density to capture the variety of possible bridge configurations, avoiding bias toward particular values.

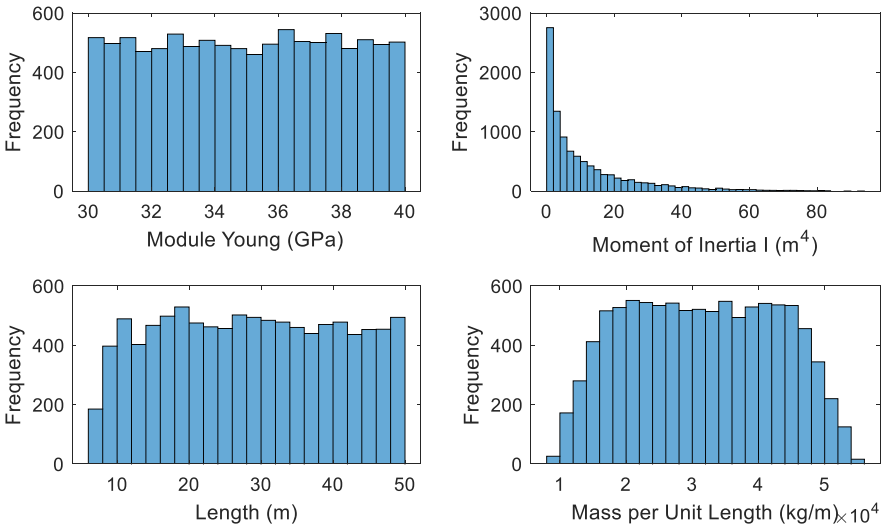

Figure 3. Histogram of Input Features: Module Young, Moment of Inertia, Length, Mass per Unit Length

Figure 4 illustrates the relationship between mass per unit length and length, revealing how these variables are distributed across these bridges. The colour intensity corresponds to the density of data points, providing insight into common structural properties within the dataset.

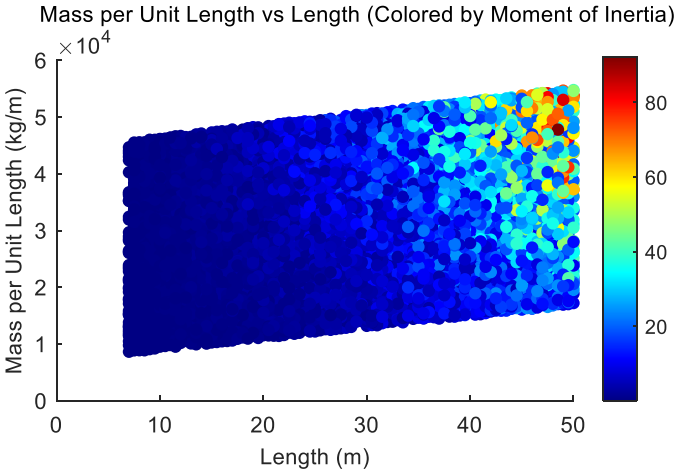

Figure 4. Mass per Unit Length vs Length Relationship, with Color Scale Indicating Moment of Inertia (m⁴)

Figure 5 summarises the first natural frequency distribution of the 10,000 bridges plotted in logarithmic terms against length (m), with upper and lower bounds delineated according to Eurocode 1 [28]. This graph highlights the natural frequency range expected for typical bridge designs and showcases the bounds within which most bridges' natural frequencies lie, ensuring compliance with Eurocode guidelines for dynamic performance.

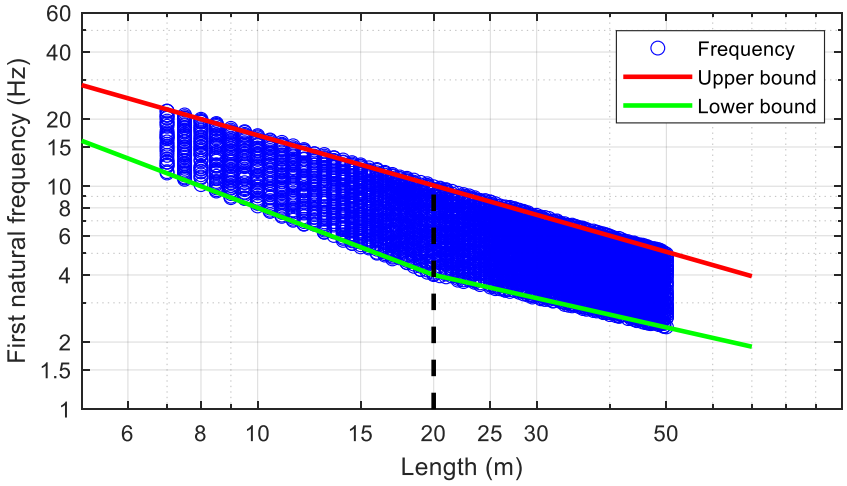

Figure 5. First Natural Frequency Distribution of 10,000 Bridges Plotted in Logarithmic Terms Versus Length (m) With Upper Bound and Lower Bound According to Eurocode 1 [28]

2.3 Data for Validation and Application Process

The developed surrogate model was validated by examining its predictive performances against the dynamic behaviours of two real bridges that were not included in the generated data for model training. The initial focus is on the Antoing Bridge near the French-Belgian border, on the high-speed railway network connecting Paris with Brussels. This multi-span structure features simply-supported prestressed concrete (PC) girders with U-shaped sections of 50 meters. The bridge's dynamic properties were obtained through extensive real-world measurements by Xia *et al.*[16]. The second bridge is a 30-meter span, simply-supported box girder bridge designed for the UK's High Speed 2 (HS2) project [49].

Error! Reference source not found. illustrates a typical overpass configuration within the two selected bridges.

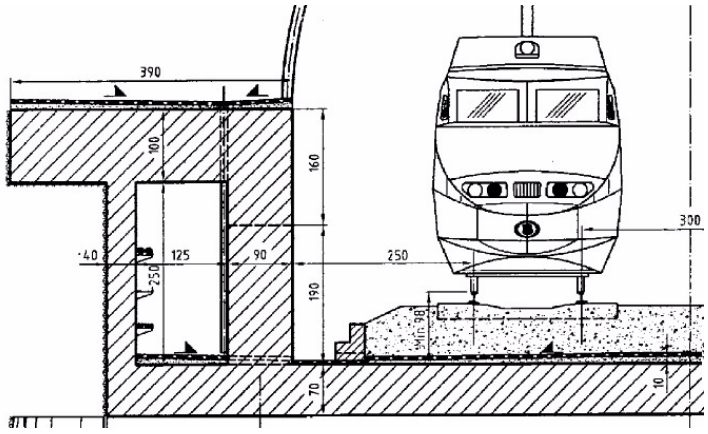

(a)

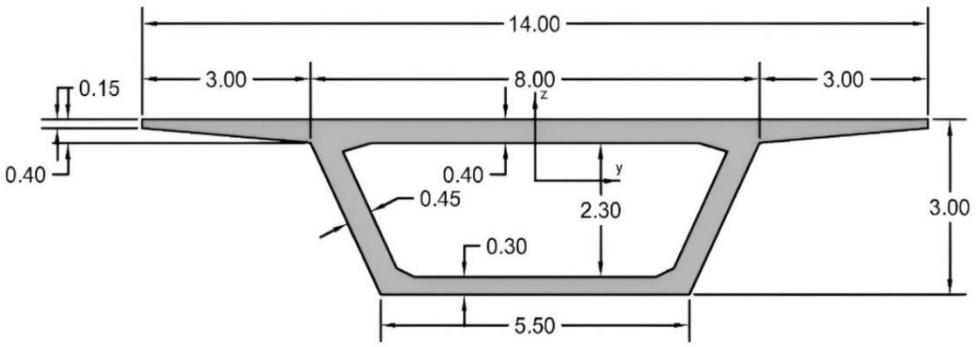

(b)

Figure 6. Cross-sectional configurations of the validation case studies: (a) Antoing Bridge - a prestressed concrete (PC) girder with U-shaped sections [16]; (b) Typical simply supported box girder bridge from UK's High Speed 2 (HS2) project [49]

For the latter bridge type—prestressed concrete box girders, we examined the design protocol used by HS2 for dynamic analysis requirements. This strategic protocol, as implemented by Pere Alfaras, Principal Bridge Engineer at Arcadis UK [49], follows the assessment framework defined in BS EN 1991-2:2003 [28] (Figure 7), which dictates when dynamic analysis is required for railway bridges.

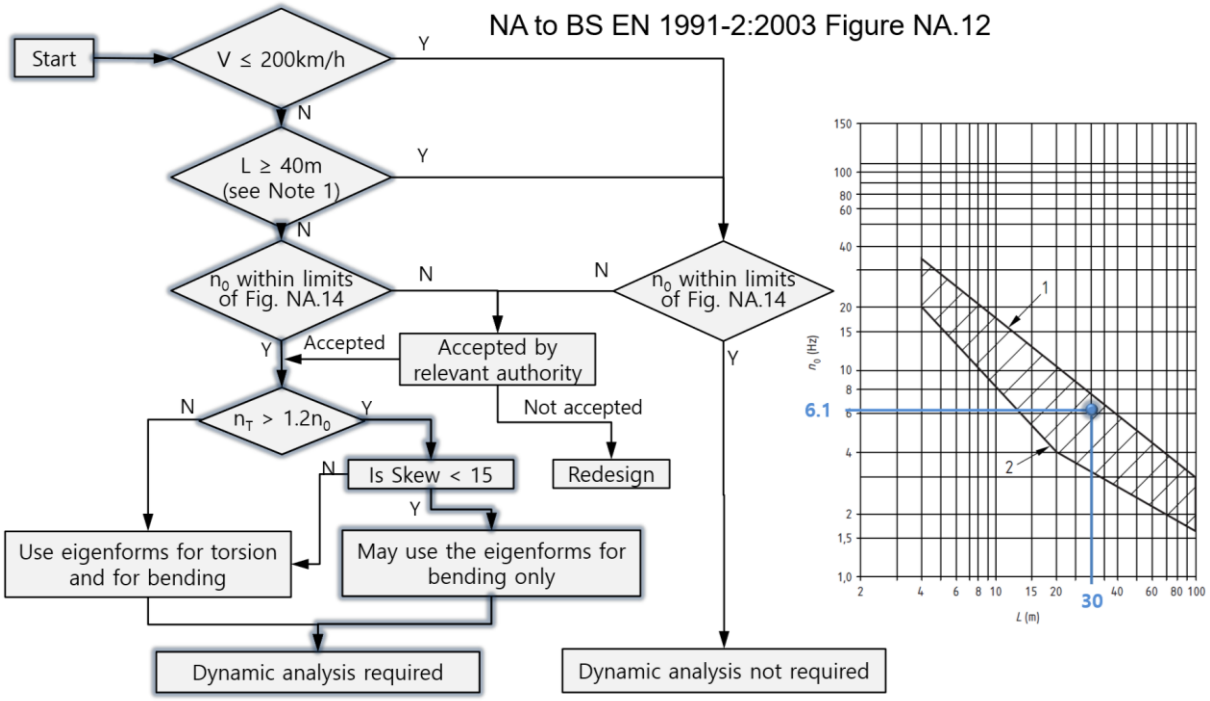

Figure 7. Process to evaluate whether the bridge requires a dynamic analysis

As part of validating our model with the HS2 bridge case study, we examined its first natural frequency of 6.1 Hz at a 30m span length against this Eurocode framework. For the HS2 bridge case, its frequency falls within the acceptable bounds, as shown in the right-hand graph. While its span length is less than 40m, dynamic analysis is required due to operational speeds exceeding 200 km/h. By validating our surrogate model against a real bridge that requires dynamic analysis according to Eurocode standards, we demonstrate its practical value as an efficient alternative to traditional analysis methods while

maintaining compliance with code requirements. The accurate prediction of dynamic responses for the HS2 bridge (detailed in Section 3.1.2) confirms our model's reliability for cases where Eurocode mandates dynamic analysis.

2.4 Surrogate Model Development

2.4.1 Indexing and Semantic Search

The bridges were divided into groups, each stored in a separate file (*.mat). This division is semantically meaningful, as it organises bridges into manageable sets for faster retrieval. When querying data for a specific bridge, instead of traditional index identification, a semantic search query is processed. The input values (descriptors of the bridge) are analysed semantically to compute a query vector, which is then used to navigate through the semantic index to identify the most contextually relevant .mat file(s).

Semantic search in this context is about finding the most relevant dataset for a given bridge based on a semantic understanding of the query, rather than a direct lookup. This involves interpreting the query's semantic context — in this case, identifying which group of data (group) a specific bridge belongs to. The semantic indexing is reflected in how the data is organised and accessed.

This approach offers several computational benefits over traditional methods:

1. Improved efficiency: Search times are significantly reduced compared to conventional database queries, as the system quickly narrows down the relevant data from the extensive 4-million-point database.
2. Enhanced accuracy: By understanding the context of bridge parameters, the search retrieves more relevant data points, potentially leading to improved prediction accuracy.
3. Scalability: As the database grows, the semantic search maintains its efficiency, unlike traditional methods that might slow down with larger datasets.

The implementation involves converting bridge characteristics into high-dimensional semantic vectors (embeddings) that capture their engineering relationships. These embeddings are then indexed using an efficient nearest-neighbor search algorithm. When analysing a new bridge, its parameters are similarly embedded, and the system rapidly identifies the most relevant existing data points.

2.4.2 Value Decoding and Estimation

The decoding process translates raw data into meaningful parameters that can be used to estimate the maximum acceleration (A_{max}), which involves several mathematical operations:

Data reshape:

$$D_k = \text{reshape}(D(k - (g-1) \times 500, :), 410, 8)$$

where D represents the original data matrix, k is the unique identifier for a specific bridge, g is the group to which the bridge belongs. The reshape function then reorganises this row into a new matrix with dimensions 410 by 8.

The factor variable scales the raw acceleration data based on the bridge's characteristics and comparison to standard parameters *(E_0, I_0)*.

$$f = \frac{D_k(3,2) \times D_k(3,3)}{E_0 \times I_0}$$

D_k is the matrix derived from the original data set, specific to a certain bridge, where $D_k(i,j)$ correspond to specific properties of interest (e.g., material properties, geometric dimensions, etc.). E_0 and I_0 are constants representing the standard values of elasticity and moment of inertia, respectively, against which the bridge data is being normalised.

The workflow depicted in Figure 8 illustrates a sophisticated approach for developing surrogate models to estimate the maximum displacement and acceleration of prestressed concrete railway bridges.

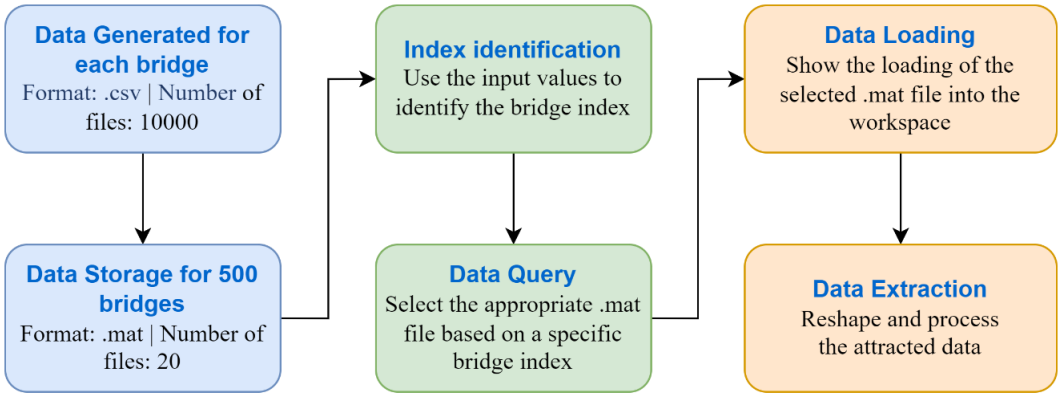

Figure 8. Surrogate Model Development and Data Manipulation Workflow

The surrogate model employs semantic search with nearest neighbor analysis to predict dynamic responses for new bridge configurations. When a query with new bridge parameters is received, the model first normalizes these parameters using the same scaling factors applied to the training data. It then computes a semantic similarity metric based on both geometric properties (span length, cross-sectional dimensions) and physical parameters (mass, stiffness, natural frequency). The K nearest neighbors (K=5) from our database are identified using this metric. Rather than selecting a single closest match, the model performs weighted interpolation between these neighbors, with weights inversely proportional to their semantic distance from the query point. This interpolation considers the physical constraints of bridge dynamics to ensure predictions remain within realistic bounds. For example, if a bridge's parameters fall between two known cases with maximum accelerations of 2.1 m/s² and 2.4 m/s² respectively, the model will predict an intermediate value based on the relative similarity to each case while respecting the underlying physical relationships. The model's accuracy is evidenced by its high R^2 values (0.999) when validated against FEM results for real bridge cases.

2.5 Generative Design Process for Cross-Sectional Optimisation

The research yielded a proposed generative design approach as a significant outcome. It skilfully combines automated data processing with human's expertise evaluation. The generative design initiative

aims to comply with the vertical acceleration criterion set by the Eurocode for ballasted track bridges, which restricts acceleration to 3.5 m/s². This criterion is established to prevent ballast destabilization, which can compromise the track's structural integrity and stability at high speeds. The objective of the method is to ensure that the vertical acceleration remains below this limit by minimising the bridge's weight and ensuring the design's reliability through human intervention based on expertise.

Figure 9 outlines the proposed generative design framework for cross-sectional optimisation, combining computational efficiency with professional insights.

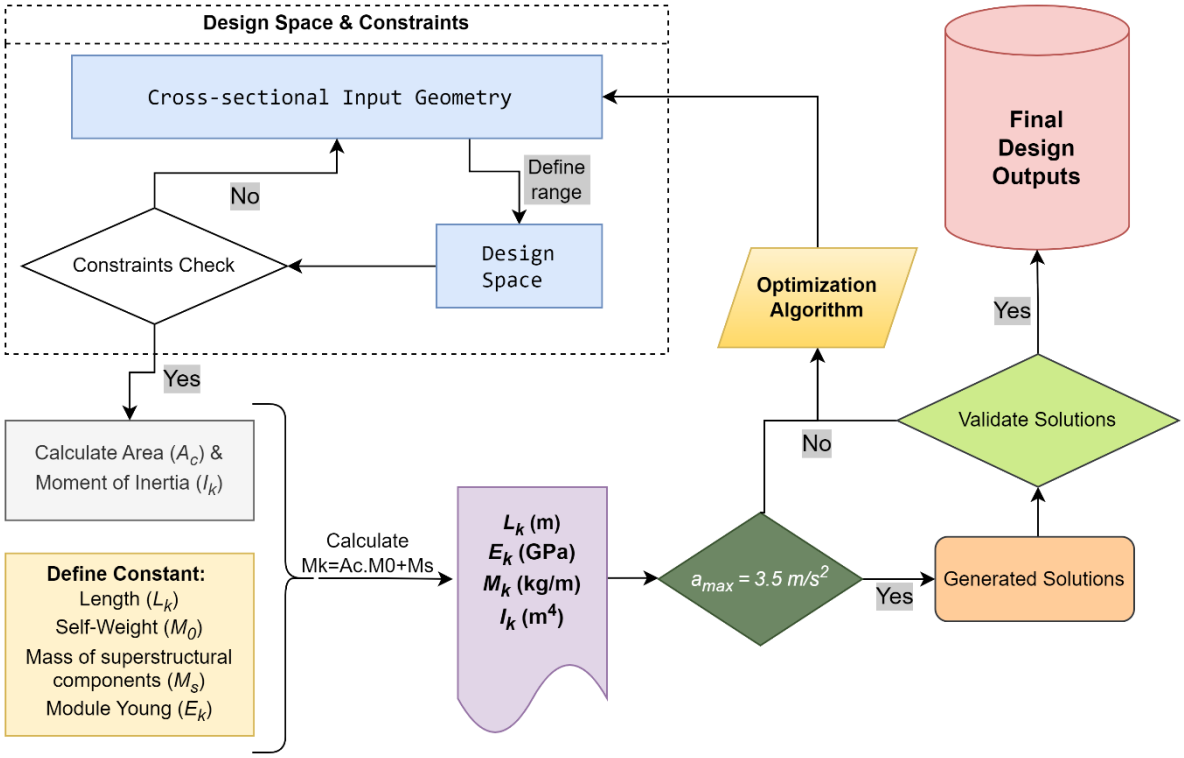

Figure 9. Flowchart of the proposed Generative Design Process for Cross-Sectional Optimisation

Definition of Input Variables with Constraints: The procedure begins by defining an initial design space that includes the bridge's dimensions, elastic modulus (E), precise cross-section geometry, and mass per unit length. Every input variable is allocated a value that allows for generating a wide range of output combinations while staying within the limits of realistic practicality. For instance, the web thickness must be at least 30 cm and should not exceed 60 cm.

Initialisation of NSGA-II Algorithm: The optimisation process commences with the initialisation of the NSGA-II algorithm [50]. This multi-objective optimisation algorithm begins with a randomly generated initial population of potential cross-sectional designs, each representing a possible solution within the defined design space.

Optimisation Loop: Central to the generative design process is the iterative optimisation loop, wherein each generation of design solutions is rigorously evaluated and evolved. Within this loop, the following steps are iterated:

- Calculate Vertical Acceleration: The vertical acceleration for each design is computed using the

surrogate model.

- Apply Genetic Operators: Genetic operators—selection, crossover, and mutation—are applied to the population of designs to explore the design space and generate new design variants.
- Fitness Evaluation: The fitness of each design is evaluated based on its vertical acceleration and mass efficiency. Designs that yield lower accelerations and reduced mass are favoured, aligning with performance and cost-effectiveness optimisation objectives.
- Convergence Check: The process checks for convergence, determining whether the design solutions have reached a state of optimality as defined by the algorithm's stopping criteria.

Optimal Design Selection: The possible alternatives that meet the maximum acceleration limitation (e.g., 3.5 m/s^2) will be chosen from the generated solutions for the following phase, which requires human experience.

Design Analysis and Selection for Validation: The final phase involves a detailed analysis of the selected designs from the previous step. Each solution must be analysed based on project requirements, considering cost, structural performance, site execution, and environmental impact. The designs that show the most potential and meet the specific criteria of the project are chosen for additional analysis and empirical validation.

2.6 Limitations and Assumptions of the Generative Design Process

While the proposed generative design framework aims to optimize the cross-sectional geometry of prestressed concrete railway bridges, it is important to acknowledge certain limitations and assumptions:

1. Shear deformability: The current model does not account for shear deformability effects, which can be significant in short-span bridges or bridges with low height-to-span ratios.
2. Transverse flexibility: The optimization process focuses primarily on longitudinal behavior and does not explicitly consider transverse flexibility, which may affect the distribution of stresses in wide bridge decks.
3. Torsional effects: While torsional resistance capacity is mentioned as a key effect, the current optimization framework does not explicitly model or optimize for torsional behavior.

While this study demonstrates the framework's application through a box girder bridge case study, the surrogate model's underlying parameters (mass, stiffness, frequency) are generic and could be applied to optimize various bridge deck types appropriate for different span ranges. Future work could extend this framework to include cross-section type selection as part of the optimization process.

An additional limitation of the current methodology relates to the load application model. Our calculations implement moving concentrated loads without considering their distribution through the ballast and sleepers. In reality, train axle loads applied at rail level are distributed through the track structure before reaching the bridge deck, an effect that is particularly significant for short-span bridges. While more refined approaches, such as the triangular distribution (25%-50%-25%) proposed by ERRI Report D 214/RP 9 [43], can provide more realistic results, our simplified approach yields conservative predictions of dynamic responses. This conservatism provides an additional safety margin in our design optimizations, though it may lead to slightly over-designed structures, particularly for shorter spans. Future refinements of the methodology could incorporate these load distribution effects to achieve more

economical designs while maintaining safety requirements.

3 Surrogate model validation and implementation

3.1 Validation of the Surrogate Model

The surrogate model's validation is an essential step to verify its accuracy and reliability in simulating the dynamic behaviour of railway bridges. This section details a methodical comparison between the surrogate model's predictions and FEM results for two actual bridges: Antoing Bridge and one from the High Speed 2 (HS2) railway line. The focus is on two critical dynamic response parameters: maximum displacement and acceleration, evaluated over a spectrum of train speeds using HSLM-A train models.

3.1.1 Antoing Bridge

Dynamic analyses were performed on Antoing Bridge to assess the developed surrogate model's predictions against FEM-derived maximum displacement and acceleration responses. Figure 10 presents a detailed comparison of the maximum displacement and acceleration experienced by the Antoing Bridge as a function of train speed, analysed using 10 different HSLM-A train models. The figure comprises two graphs, one depicting displacement and the other acceleration, with each graph displaying a series of peaks corresponding to the different train models.

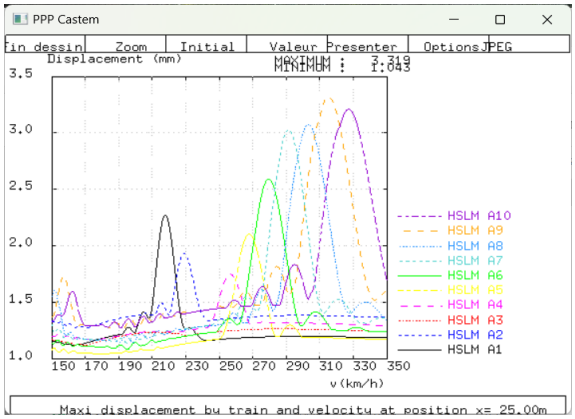

(a) Displacement results by KD-Railway

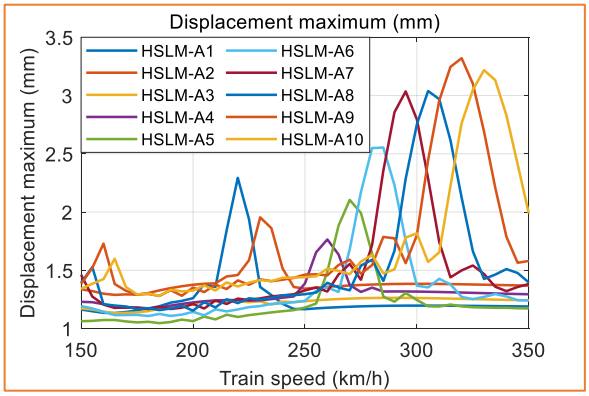

(b) Displacement results by surrogate model

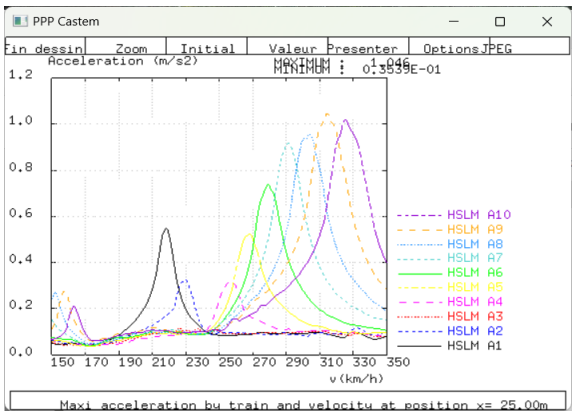

(c) Acceleration results by KD-Railway

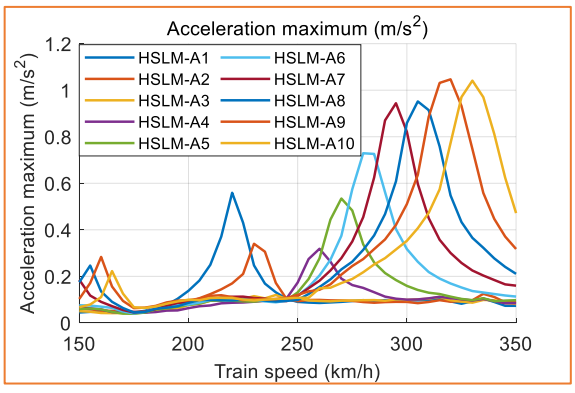

(d) Acceleration results by surrogate model

Figure 10. Antoing Bridge - Comparison of Maximum Displacement and Maximum Acceleration using KD-Railway-based Cast3M and developed model

Figure 11 offers a quantitative validation using a scatter plot of the maximum displacement and acceleration as predicted by the surrogate model against the FEM results for various HSLM-A train models. The left graph illustrates the comparison for maximum displacement (in mm), while the right graph does the same for maximum acceleration (in m/s²). Both graphs include a "Perfect Line" which represents an ideal 1:1 correlation between the surrogate model and FEM results. Most data points are closely aligned along the Perfect Line, falling within a narrow band that represents a ±5% error margin for both maximum displacement and acceleration responses.

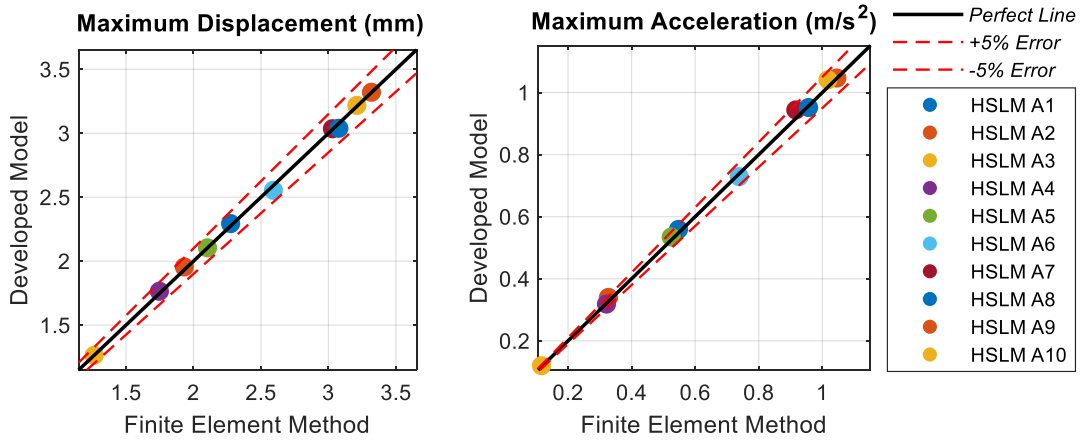

Figure 11. Comparison of Maximum Displacement and Maximum Acceleration at the point at the middle span of the Antoing Bridge subjected to 10 conventional train models using FEM and developed model

3.1.2 HS2's bridge

The validation process extended to the HS2 Bridge. Similarly, comparative dynamic analyses were conducted using both the KD-Railway-based Cast3M software and the developed surrogate model. Figure 12 presents plots that compare a range of train speeds for different HSLM-A models, illustrating the surrogate model's fidelity in reproducing the dynamic responses. These responses are consistent with those from the FEM, even across varying train speeds and models, indicating the model's robustness.

Figure 13 directly compares the maximum displacement and acceleration of each bridge subjected to 10 train models. The data points, when plotted against the Perfect Line, primarily lie within the ±5% error bars, indicating a strong connection between the surrogate model and FEM results. The uniformity observed in several train models highlights the surrogate model's capacity to accurately represent a diverse range of dynamic reactions.

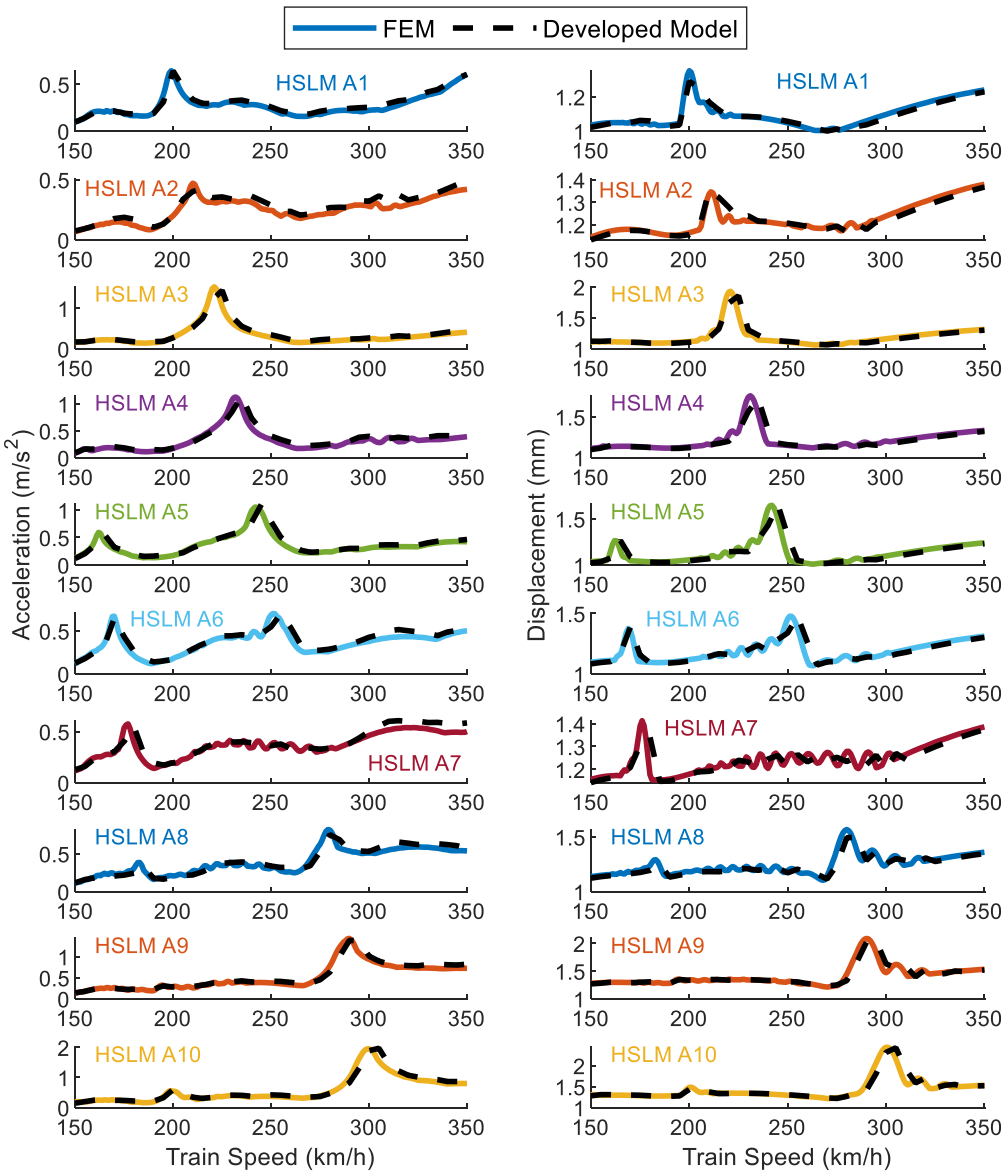

Figure 12. HS2 bridge - Comparison of Maximum Displacement and Maximum Acceleration using KD-Railway-based Cast3M and developed model

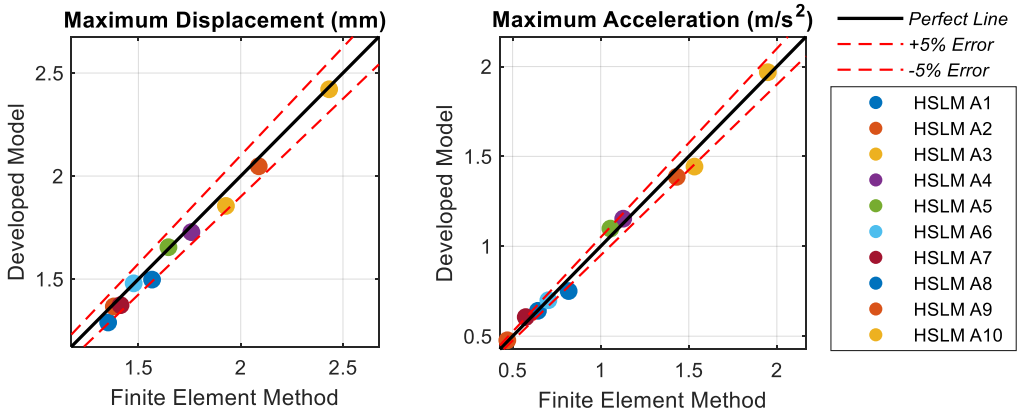

Figure 13. Comparison of Maximum Displacement and Maximum Acceleration at the point at the middle span of the HS2's Bridge subjected to 10 conventional train models using FEM and developed model

3.2 Enhanced Validation and Future Development Directions

In the validation phase, only the singular maximum displacement or acceleration values were compared for each bridge subjected to train models moving within the speed range of [150, 350] km/h. However, to derive a more detailed dynamic profile, this section will adopt a more comprehensive validation approach by comparing the spectrums results. Specifically, 41 discrete data points representing the maximum displacement and acceleration corresponding to each incremental speed within the speed range, with a step of 5 km/h, will be used. In total, 410 values of displacement and 410 values of acceleration will be compared for each bridge.

The comparison between the values predicted by the surrogate model and those obtained via FEM is illustrated in Figure 14. Notably, the surrogate model exhibited a commendable predictive accuracy for acceleration, with an error margin under 5%.

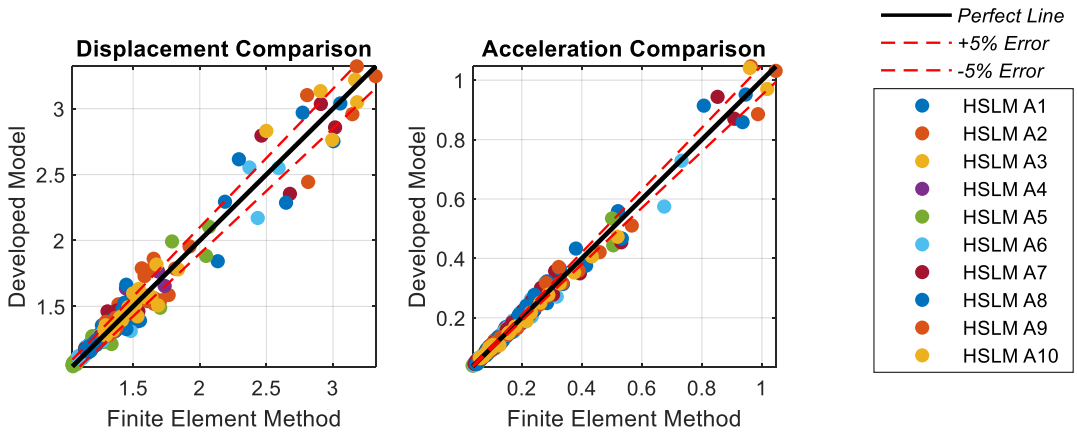

(a) Antoing Bridge

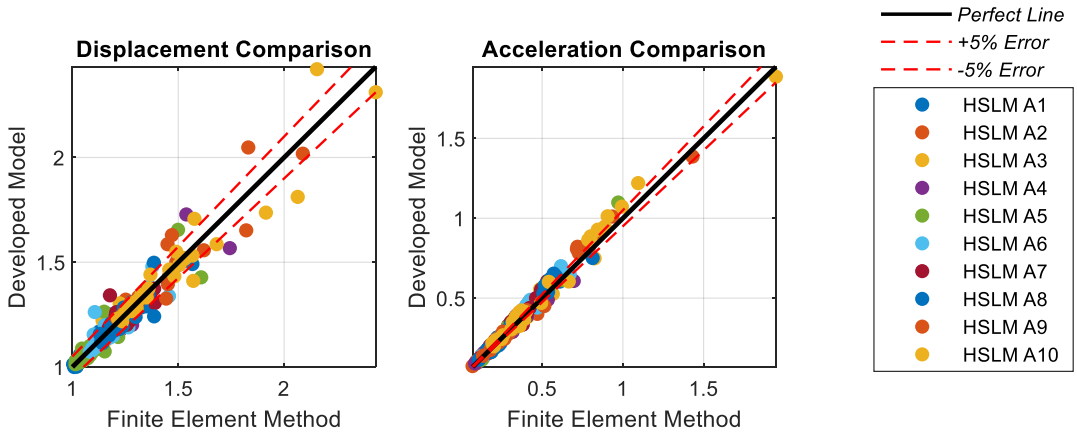

(b) HS2's bridge

Figure 14. Comparison of envelop displacements and acceleration of two bridges subjected to10 conventional train models using FEM and developed model

The performance metrics of the predictions are summarised in Table 2, with the surrogate model achieving an R^2 of 0.99 and RMSE below 0.045 for the maximum acceleration and displacement values. When evaluating the complete set of data points for the envelope curves (410 values), the predictive

performance remains strong, with R^2 of 0.96 and 0.93 for displacement predictions for the Antoing and HS2 bridges, respectively. Acceleration predictions are notably accurate, with R^2 of 0.99 and 0.97 for the Antoing and HS2 bridges, respectively.

Table 2. Prediction performance metrics on envelop and maximum acceleration and displacements for Antoing and HS2 bridges

		R-squared	RMSE	MAE
Antoing Bridge	Envelop Displacement	0.964	0.02	0.011
	Maximum Displacement	0.999	0.02	0.015
	Envelop Acceleration	0.987	0.075	0.037
	Maximum Acceleration	0.998	0.013	0.011
HS2 Bridge	Envelop Displacement	0.926	0.045	0.026
	Maximum Displacement	0.984	0.043	0.035
	Envelop Acceleration	0.971	0.036	0.028
	Maximum Acceleration	0.991	0.043	0.033

Building on the current findings, there are several promising directions for advancing the research and develop other surrogate models. First, increasing the detail in the dataset could refine the model's accuracy. If the speed interval is narrowed from 5 km/h to 2 km/h or even 1 km/h, more data could be created. This data will provide more insights of how bridges behave under different speeds. For instance, with a 2 km/h speed interval, the model would generate 101 discrete outputs for vertical displacements for a single train model, considering each bridge within the speed range from 150 to 350 km/h.

Furthermore, expanding the range of speeds could also improve its usefulness. If the upper speed limit is increased up to 450 km/h, the model would be better suited for future high-speed rail developments. The same methodology can be applied to a wider variety of bridge designs, such as continuous, short-span, and skew bridges.

Future research could also enhance the current methodology by incorporating more sophisticated modeling approaches. Particularly, the inclusion of detailed train-track-bridge interaction models and improved representation of rail irregularity effects could enhance acceleration prediction accuracy. While the current HSLM-A model with the $\varphi''/2$ coefficient provides a practical approach aligned with Eurocode standards, more comprehensive modeling of track irregularities could further improve the surrogate model's predictive capabilities, especially for acceleration responses. This enhancement would be particularly valuable for cases where detailed acceleration analysis is critical for design decisions.

Finally, a wide range of damping ratios could be considered rather than a fixed value since different bridges react differently. A more flexible approach to damping could give us more precise results, making the model even more reliable for predicting bridge behaviour.

3.3 Practical Implementation: Fast KD-Railway for Rapid Dynamic Analysis

The surrogate model's performance across different HSLM-A train models and speeds indicates its potential as a practical tool in engineering analysis and design of railway bridges, providing a computationally efficient alternative to traditional FEM without compromising accuracy. In the context

of rapid dynamic analysis, the surrogate model has been integrated into the KD-Railway software recently developed by authors [41], serving as an autonomous module that obviates the necessity for the Cast3M open-source code. This integration furnishes users with an alternative for independent operation.

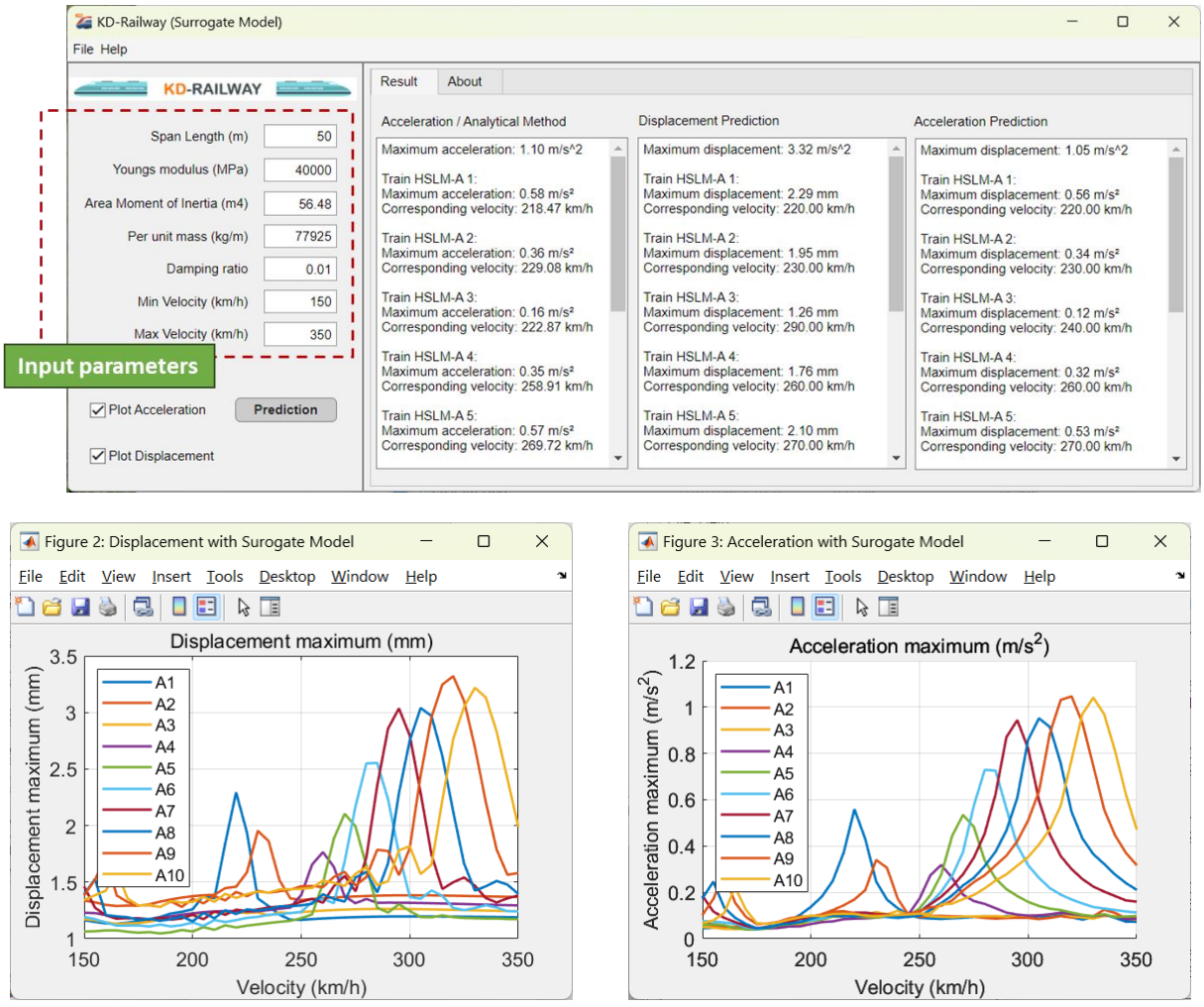

Figure 15. Fast KD-Railway User Interface and Dynamic Results of Antoing Bridge Using Developed Fast KD-Railway Tool

The interface of the Fast KD-Railway tool is presented in Figure 15. The surrogate model's predictive functionality, specifically for maximum vertical acceleration and maximum vertical displacement, has been integrated into the updated version, which is composed of an area for defining the input parameters and an area for result display:

- Input Parameter Definition Area: This interface segment allows input of the bridge's parameters, setting the stage for the subsequent analysis.
- Selection Area: Users can switch between graphical and textual result formats, offering flexibility in result presentation.
- Text-based Result Display Area: This section presents a tabulated view of dynamic response metrics, listing the maximum accelerations experienced by the bridge under HSLM-A train traversals, along with the corresponding speeds, all formatted for ease of data extraction and report integration.

- Image-based Result Display Area: By activating the "Plot Results" function, users can graphically represent the results, facilitating a more intuitive analysis and interpretation of the data.

The Fast KD-Railway software represents a significant advancement in the field of dynamic analysis of bridges by offering a marked reduction in model development time compared to FEM simulation tools such as Midas, Abaqus, or Robot Structural Analysis. Traditional FEM software necessitates a full working day to construct a model capable of dynamic analysis. Moreover, these conventional methods require extensive manual data interpretation whenever input parameters are varied, contributing to the protracted timeframes for model adjustment and analysis [41].

A comparative analysis of computational efficiency reveals significant improvements in calculation time across different methods for dynamic analysis of railway bridges. This comparison is particularly relevant when considering the comprehensive evaluation required by Eurocode standards, which necessitates 1510 simulations across 10 HSLM-A train models and speed ranges from 100 to 400 km/h. Traditional Finite Element Method (FEM) analysis, using software like ANSYS, requires approximately 22 minutes for a single bridge analysis. The KD Railway software, developed as an intermediate improvement, substantially reduces this simulation time to about 20 seconds per analysis. However, the proposed surrogate model further diminishes the calculation time to approximately 0.1-0.5 seconds per analysis. This represents a remarkable reduction in computation time compared to traditional FEM methods, from 22 minutes to as low as 0.1 seconds. Such near-instantaneous computation enables extensive simulations and iterative design processes that were previously impractical due to time constraints. Crucially, this significant gain in efficiency does not compromise accuracy. The surrogate model's precision has been rigorously verified against real-world structures, including the Antoing bridge (please see the section 4), demonstrating its reliability for practical applications in railway bridge design and analysis.

4 Case study: Cross-Sectional Generative Design

4.1 Problem description

In this section, the generative design framework described in Section 2.5 will be used to refine design parameters for the cross-sectional geometry of a standard simply-supported box girder bridge deck (Figure 16), ensuring efficient and effective solutions. The design process considers two primary conditions affecting the bridge deck's cross-section: constructive and resistant conditions. Constructive conditions depend on the builder's experience, site conditions, and available resources, making them challenging to assess due to their variability. Resistant conditions, on the other hand, are clearer and include several key effects worth emphasising:

- Bending resistance capacity depends on the deck's height (H) and the areas of the top and bottom slab.
- Transverse flexibility and shear deformability: induce a distortion of the box, leading to an

inequality in the distribution of longitudinal bending stresses.

- Torsion resistance capacity: depends on the thickness of the box walls (*T2*) and the area enclosed by them.
- Resistance capacity of the upper slab against a direct load: significant transverse bending may occur and this depends on the separation between webs and the length of the external cantilevers (W3).

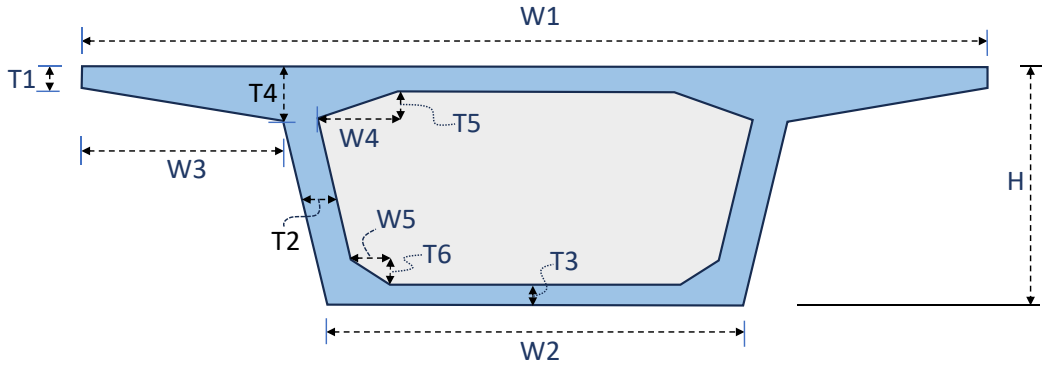

Figure 16. Cross-Sectional Dimensions and Parameters of a Structural Bridge Component

In this sense, eleven parameters of the bridge deck's cross-section can be selected as cross-sectional design input that will be optimised through the generative design framework. The range and constraints established for each parameter, the used constants, and the meticulously structured process are represented in Figure 17.

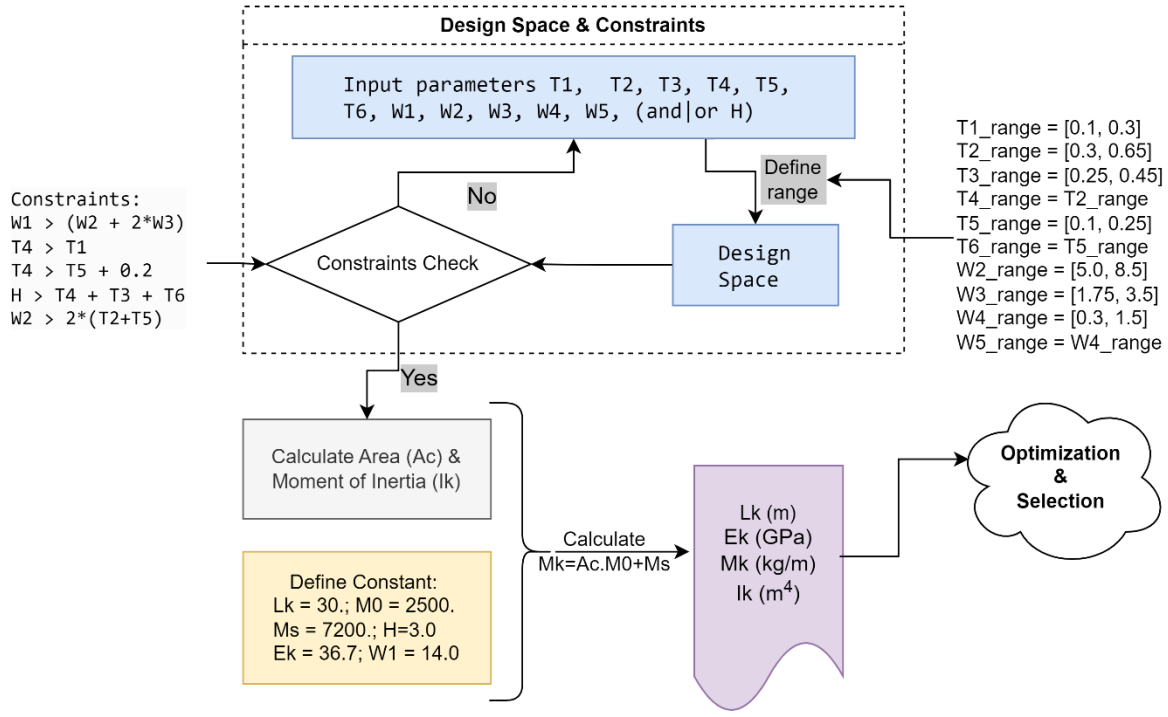

Figure 17. Cross Section, Design Space and Constraints of the Generative Design Process

The process consists of:

- **Design Space & Constraints:** The design space is initially characterised by specifying input parameters (T1-T6, W1-W5, H), which collectively define the box girder bridge's geometry. Constraints are methodically imposed to maintain design feasibility and uphold structural integrity. These include proportional relations among widths and thicknesses, such as W1 being mandated to exceed the combined widths of W2 and W3, as well as stipulating T4 as superior to T1. Additionally, a hierarchical constraint system ensures that T4 surpasses T5 by a quantifiable margin and that other constraints regarding H and W2 are met.
- **Constraints Verification:** Subsequently, a verification step assesses the alignment of design parameters with the imposed constraints. Non-compliance prompts a re-evaluation, necessitating an iterative refinement of parameters to achieve a viable design configuration.
- **Structural Property Computation:** Upon satisfying all constraints, the process progresses to calculate essential structural properties—area (A_c) and moment of inertia (I_k)—integral to assessing the dynamic response of the bridge.
- **Definition of Constants:** In parallel, constants are delineated: bridge span (L_k), concrete density (M_0), ballast mass per unit length (M_s), Young's modulus of concrete (E_k), and bridge width (W1). These constants serve as foundational benchmarks for the ensuing optimisation.
- **Optimisation & Selection:** The optimisation phase iteratively manipulates the design parameters within the established space to discern the optimal combination that satisfies performance criteria, such as minimising weight in keeping structural efficiency.

In the optimisation framework detailed within this study, we intentionally omitted factors like transverse flexibility, shear deformability, and torsion resistance capacity. This decision was rooted in the desire to simplify the optimisation process, acknowledging that while these elements are crucial in specific scenarios, their inclusion would unduly complicate the methodology without markedly advancing the study's core aims. We concentrated on key parameters significantly influencing the bridge's longitudinal dynamic behaviour during the initial design phase.

This generative design process is exemplified through two separate case studies, one involving ten variables and the other eleven, demonstrating its versatility and adaptability across different scenarios.

- **Case Study with 10 Variables:**
  In the first case study, ten variables (T1, T2, T3, T4, T5, T6, W2, W3, W4, W5) were used to define the cross-sectional parameters of the box girder bridge. The bridge deck's height (H) is considered constant and takes a value of 3.0 m (L/10). The absence of height parameter H in this scenario means that the design optimisation was focused on the planar cross-sectional properties without considering the variable height dimension.
- **Case Study with 11 Variables:** The second case study extended the design space to include an additional variable, height (H), thereby expanding the generative design process to consider the vertical dimension of the bridge's cross-section. This additional variable introduces a new layer of complexity, as height influences the structural behaviour in terms of overall stiffness.

Incorporating H allows for a more holistic optimisation, factoring in the effects of the bridge's elevation profile on dynamic performance and stability.

4.2 Generative design solutions

The generative design process yielded a variety of feasible solutions for each case study analysed. For instance, Figure 18 presents eleven distinct solutions derived from a case study involving ten variables. These solutions significantly diverge from the initial parameters specified in the reference section, predominantly showcasing a reduction in nearly all variable values. Such a reduction aligns with the optimisation objective of minimising the mass per unit length by reducing the cross-sectional area. Importantly, all proposed solutions comply with the Eurocode requirement that the bridge deck's maximum acceleration does not exceed 3.5 m/s². Nonetheless, as a direct consequence of the reduced mass per unit length, the acceleration in each solution is naturally higher compared to the reference scenario.

To further elucidate the results, it is noteworthy that the thickness parameters (T1-T4) and width parameters (W2-W3) consistently show lower values across all optimized solutions compared to the reference design. This trend indicates that the generative design algorithm effectively explores the design space to find more efficient cross-sectional geometries. The cross-sectional area (A_c) and moment of inertia (I1) also decrease accordingly, reflecting the overall reduction in material usage.

Solution $V10_{17}$, for example, achieves the lowest mass per unit length (Mk) while still maintaining structural integrity and meeting the acceleration criterion. This solution represents a significant optimization, with a mass reduction of approximately 30% compared to the reference design. However, it is crucial to note that this mass reduction comes with a trade-off, as the maximum acceleration (a_{max}) for this solution approaches the 3.5 m/s² limit.

Interestingly, the solutions exhibit a range of trade-offs between mass reduction and dynamic performance. Solutions $V10_{09}$ to $V10_{16}$ offer varying degrees of mass reduction with corresponding increases in maximum acceleration, allowing designers to choose the most appropriate balance for specific project requirements. This spectrum of options demonstrates the power of the generative design approach in providing multiple viable alternatives, each with its own set of advantages in terms of material efficiency and dynamic behavior.

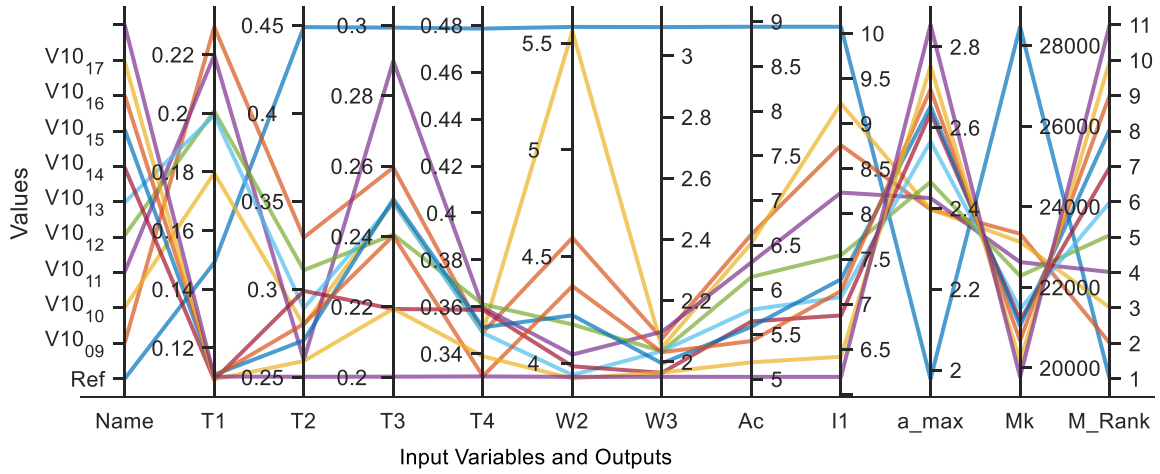

Figure 18. Feasible Solutions for the Generative Design Process with 10 Input Variables

In the second case study, as depicted in Figure 19, fifteen viable solutions were identified, with the deck height *(H)* being included as a design variable. Of these solutions, six feature a deck height exceeding the reference model, while the remaining nine solutions exhibit a reduced height, as detailed in Table 2. Consistent with findings from the case study involving ten variables, a reduction in the values of the other ten variables was also observed. This approach aligns with the objective of minimising mass per unit length, reflecting the optimisation trends observed in the preceding analysis.

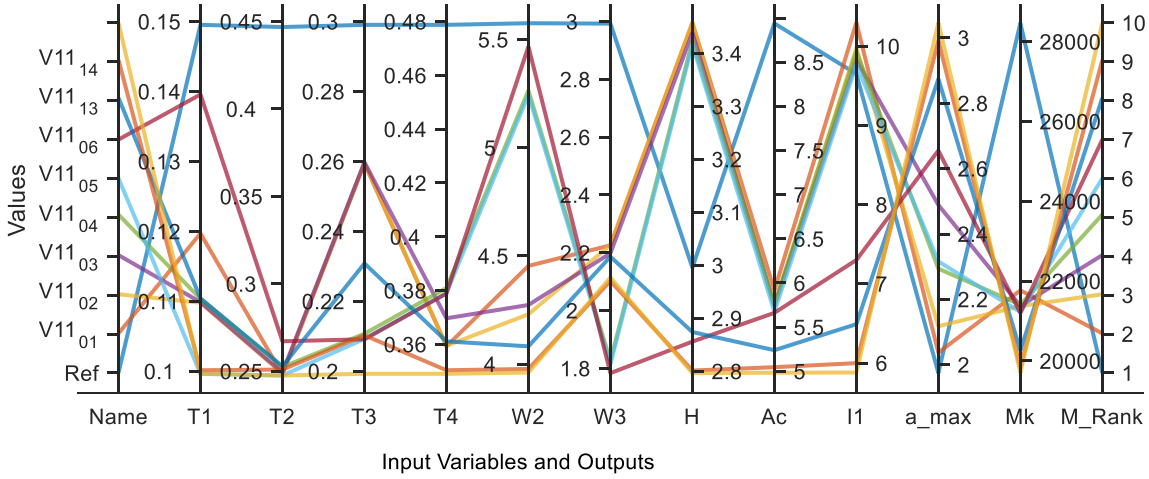

Figure 19. Feasible Solutions for the Generative Design Process with 11 Input Variables

Upon closer examination of Figure 19, several notable patterns emerge. The inclusion of deck height *(H)* as a variable introduces an interesting dynamic to the optimization process. Solutions $V11_{01}$ to $V11_{05}$ showcase increased deck heights compared to the reference model, ranging from approximately 3.4m to 3.46m. This increase in height allows for a more significant reduction in other dimensional parameters, particularly the thickness variables (T1-T4) and width variables (W2-W3).

Interestingly, the solutions with increased deck height tend to achieve lower mass per unit length (M_k) while maintaining relatively low maximum accelerations (a_{max}). Solutions $V11_{06}$ to V11_15 demonstrate

651 that viable designs can also be achieved with reduced deck heights, some as low as 2.64m. These
652 solutions generally show less dramatic reductions in other variables, indicating a trade-off between
653 height reduction and the need to maintain adequate cross-sectional properties for structural integrity.

654 The moment of inertia (I_1) values vary significantly across the solutions, reflecting the complex interplay
655 between deck height and other cross-sectional dimensions. Solutions with higher deck heights tend to
656 maintain higher I1 values, contributing to their improved dynamic performance despite reduced mass.

657 **Table 3. Selected solutions for the Generative Design process with 10 and 11 variables**

Name	T1	T2	T3	T4	T5	T6	W2	W3	W4	W5	H	Area	I1	a_max	M_k
Reference	0.15	0.45	0.30	0.48	0.05	0.15	5.50	3.00	0.50	0.30	3	8.96	10.09	1.98	29566
Validated design for Optimisation process with 10 variables															
V10_01	0.20	0.38	0.29	0.40	0.11	0.25	6.06	2.09	1.03	1.13	3	8.08	11.11	2.09	27398
V10_02	0.28	0.38	0.41	0.38	0.12	0.25	4.49	2.02	1.06	0.62	3	7.93	10.63	2.12	27031
V10_03	0.17	0.33	0.36	0.42	0.11	0.25	4.26	1.97	1.23	0.67	3	7.76	10.00	2.20	26597
V10_04	0.26	0.34	0.27	0.41	0.12	0.25	4.23	2.01	1.06	1.19	3	7.44	9.18	2.22	25807
V10_05	0.26	0.33	0.26	0.40	0.12	0.25	4.19	1.98	0.84	1.19	3	7.19	9.01	2.26	25176
V10_06	0.14	0.32	0.37	0.35	0.12	0.25	4.65	1.95	0.96	1.35	3	7.04	10.08	2.30	24790
V10_07	0.17	0.34	0.26	0.40	0.12	0.25	4.09	1.89	0.66	0.50	3	6.93	8.40	2.37	24528
V10_08	0.17	0.35	0.39	0.34	0.13	0.25	4.28	2.01	0.85	0.41	3	6.75	9.41	2.40	24084
V10_09	0.23	0.33	0.26	0.35	0.12	0.25	4.31	1.98	0.59	1.15	3	6.63	8.77	2.45	23772
V10_10	0.18	0.28	0.25	0.35	0.11	0.25	5.47	1.95	0.71	0.98	3	6.53	9.23	2.45	23534
V10_11	0.22	0.26	0.29	0.36	0.12	0.25	3.65	2.00	0.68	1.06	3	6.31	8.24	2.48	22965
V10_12	0.20	0.31	0.24	0.36	0.13	0.25	3.81	1.93	0.80	0.61	3	6.13	7.53	2.52	22535
V10_13	0.20	0.29	0.25	0.35	0.13	0.25	3.54	1.94	0.58	0.41	3	5.79	7.09	2.64	21677
V10_14	0.11	0.30	0.22	0.36	0.13	0.24	3.59	1.87	0.39	0.48	3	5.66	6.89	2.72	21362
V10_15	0.11	0.27	0.25	0.35	0.13	0.24	3.86	1.89	0.51	0.47	3	5.57	7.26	2.73	21137
V10_16	0.11	0.28	0.24	0.33	0.13	0.24	4.03	1.93	0.33	0.39	3	5.42	7.14	2.78	20747
V10_17	0.11	0.26	0.22	0.34	0.13	0.24	3.52	1.87	0.33	0.41	3	5.20	6.43	2.85	20211
V10_18	0.11	0.25	0.20	0.33	0.13	0.24	3.52	1.85	0.32	0.39	3	5.02	6.19	2.96	19740
Validated design for Optimisation process with 11 variables															
V11_01	0.12	0.25	0.26	0.36	0.14	0.21	4.15	2.23	0.53	0.86	3.46	5.93	10.89	2.04	22019
V11_02	0.11	0.25	0.26	0.36	0.15	0.21	3.88	2.23	0.45	0.96	3.46	5.75	10.48	2.12	21566
V11_03	0.11	0.25	0.26	0.37	0.17	0.21	3.93	2.20	0.44	0.72	3.44	5.75	10.29	2.49	21563
V11_04	0.11	0.25	0.21	0.38	0.18	0.23	5.11	1.82	0.34	0.48	3.42	5.74	10.4	2.29	21550
V11_05	0.10	0.25	0.21	0.38	0.18	0.23	5.10	1.82	0.34	0.48	3.42	5.69	10.2	2.32	21415
V11_06	0.14	0.27	0.21	0.38	0.18	0.24	5.37	1.79	0.39	0.57	2.86	5.68	7.15	2.66	21395
V11_07	0.11	0.25	0.26	0.35	0.16	0.21	3.88	2.18	0.41	0.68	3.45	5.66	10.17	2.52	21360
V11_08	0.17	0.27	0.21	0.37	0.15	0.22	3.83	2.11	0.41	0.54	2.79	5.55	5.88	2.69	21085
V11_09	0.11	0.26	0.21	0.38	0.18	0.24	5.31	1.78	0.37	0.51	2.64	5.4	5.81	2.73	20712
V11_10	0.11	0.25	0.26	0.36	0.16	0.22	3.65	2.06	0.44	0.80	2.72	5.34	5.77	2.75	20555
V11_11	0.10	0.25	0.20	0.38	0.18	0.24	5.10	1.77	0.33	0.49	2.77	5.32	6.21	2.81	20506
V11_12	0.10	0.25	0.20	0.38	0.18	0.24	5.04	1.78	0.32	0.50	2.64	5.24	5.53	2.97	20309
V11_13	0.11	0.25	0.23	0.36	0.15	0.22	3.69	2.18	0.38	0.52	2.87	5.22	6.09	2.87	20256
V11_14	0.10	0.25	0.21	0.35	0.16	0.22	3.57	2.10	0.37	0.54	2.80	5.04	5.49	2.99	19810
V11_15	0.10	0.25	0.20	0.35	0.16	0.22	3.56	2.12	0.37	0.51	2.80	5.00	5.37	3.05	19710

658

4.3 Discussion

In this study, a wide range of design options by setting the parameters were selected—like the width (W2) between 5 and 8.5 meters, and the thicknesses (T3 and T2) from 0.25 to 0.45 meters and 0.3 to 0.65 meters, respectively—beyond the usual limits seen in everyday bridge construction. This approach allowed to thoroughly investigate various design possibilities, pushing the limits of what's commonly done in bridge design.

However, expanding the range of these parameters means it might come up with designs that work well in theory but might not be practical due to various reasons. As a result, expert review becomes crucial during this stage.

Looking more closely at the case study (Figure 20), the bridge deck design is looked at from two perspectives, e.g., constructivity and resistance. From a construction point of view, some designs suggest very thin parts (about 0.25 meters thick), which does not comply with the construction constraints about minimal thickness, e.g., 4-5 times thicker than the prestressing sheaths. On the other hand, from a structural standpoint, designs with steeply angled or very thin parts present significant challenges. These designs might not be strong enough to resist certain types of damage, like shear, which is a concern for the overall durability of the bridge.

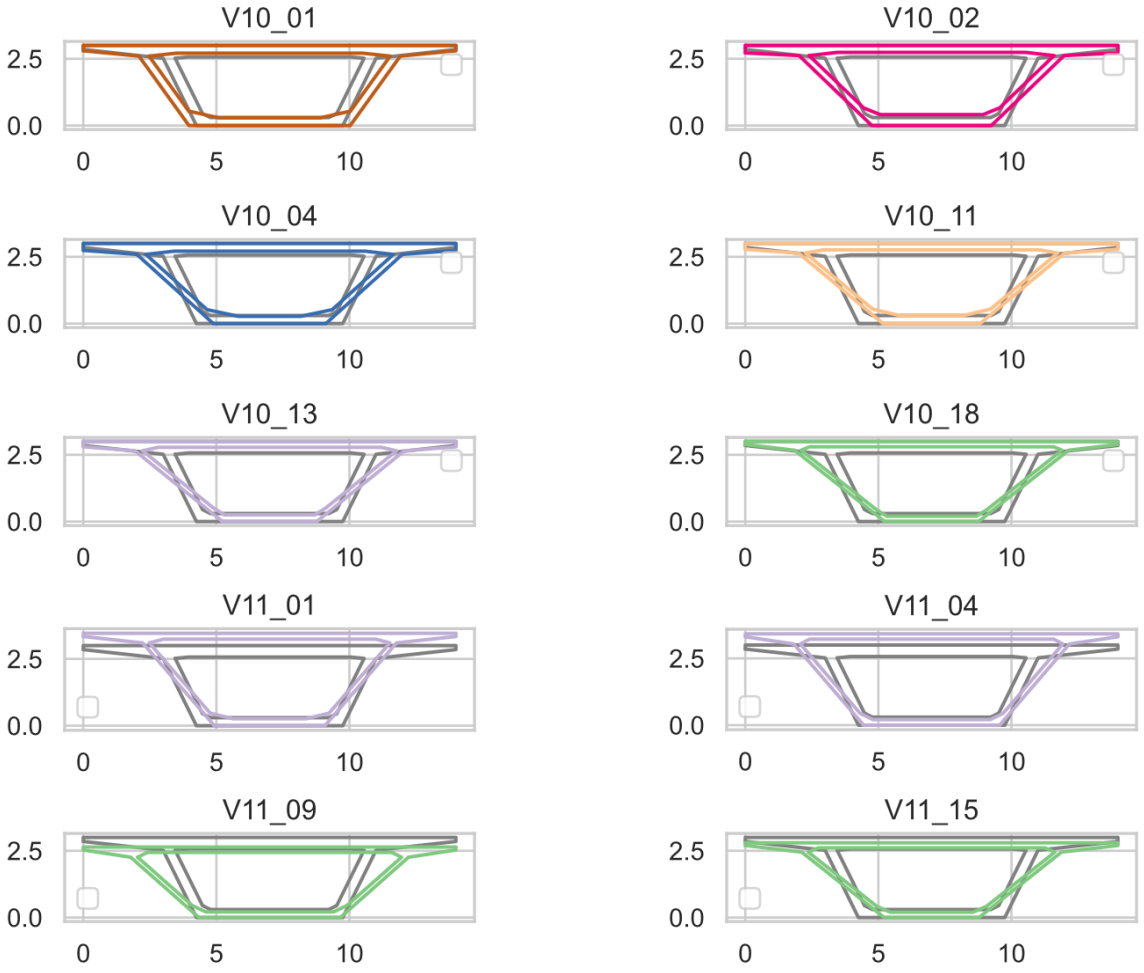

Figure 20. Representative Geometry Comparison of Selected Solutions Relative to the Reference, Coloured by Mass

per Unit Length

Furthermore, this study's primary emphasis on developing a surrogate model and introducing a generative design process meant that a detailed examination of displacement limitations was not included in our initial analysis. It's crucial to understand that the process of checking for displacement limitations entails a thorough assessment of both static and dynamic loads affecting the bridge structure. This checking ensures that the total displacement remains within the safety and serviceability thresholds set by applicable standards and codes. While this evaluation is essential for the practical implementation of bridge designs, it constitutes a separate phase of analysis that could be smoothly incorporated into our research framework in subsequent developments. Integrating this step will guarantee that the innovative designs produced through our surrogate model and generative design methodology not only demonstrate structural creativity but also comply with all relevant engineering and safety standards.

5 Conclusion

This study introduces a significant step forward in optimising high-speed railway bridge design. It highlights the crucial role of surrogate modelling, generative design, and optimisation within this domain. The compilation of an extensive database, comprising over 4 million data points for dynamic analysis, adheres to Eurocode standards and serves as a critical resource for investigating the dynamic behaviours of over 10,000 high-speed, single-span prestressed concrete railway bridges subjected to HSLM-A train loads.

The surrogate model, developed as the core of this research, featuring semantic search and advanced decoding techniques, markedly improves the efficiency and accuracy of dynamic behaviour predictions. This model has been rigorously validated across diverse bridge structures, demonstrating its broad applicability and robustness. Antoing Bridge and the HS2 project's bridge, representing both traditional and contemporary construction techniques, served as benchmarks for this validation. This facilitated a meticulous comparison of empirical data with the model's predictions, affirming the model's precision (evidenced by an R^2 value of 0.999) and its relevance to modern design practices. Through this dual analysis, the study not only verifies the model's accuracy but also illustrates its versatility in addressing various engineering challenges.

This study further introduces a novel methodology aimed at refining the cross-sectional geometry of railway bridges. Employing this methodology in a targeted case study yielded multiple designs that outperformed the original design in reducing mass per unit length. This outcome effectively demonstrates the methodology's capability to enhance the efficiency of structural design, underscoring its significant potential for optimising bridge construction practices.

Looking ahead, this study proposes several avenues for further research. These include expanding the velocity range within the database to enhance the model's applicability and accuracy and refining the selection process for bridge models to streamline data generation. Additionally, leveraging the amassed database to explore advanced machine-learning techniques could pave the way for innovative analytical

tools. Such tools could transform into accessible web applications, extending the impact of this research within the computational bridge engineering field and beyond. A complete process could be developed by incorporating comprehensive checks for displacement limitations to ensure that the designs represent structural innovation and meet all necessary standards for safety, serviceability, and compliance with engineering codes.

In essence, this research builds a bridge between advanced technology and structural optimisation, offering new perspectives for future studies in bridge design and analysis. Its contributions are poised to shape the future landscape of computational bridge engineering, emphasising efficiency, accuracy, and the integration of cutting-edge technology in the design and analysis of modern infrastructure.

Annexe

Dimensions of the section and their corresponding coordinates in the calculation of moment of inertia.

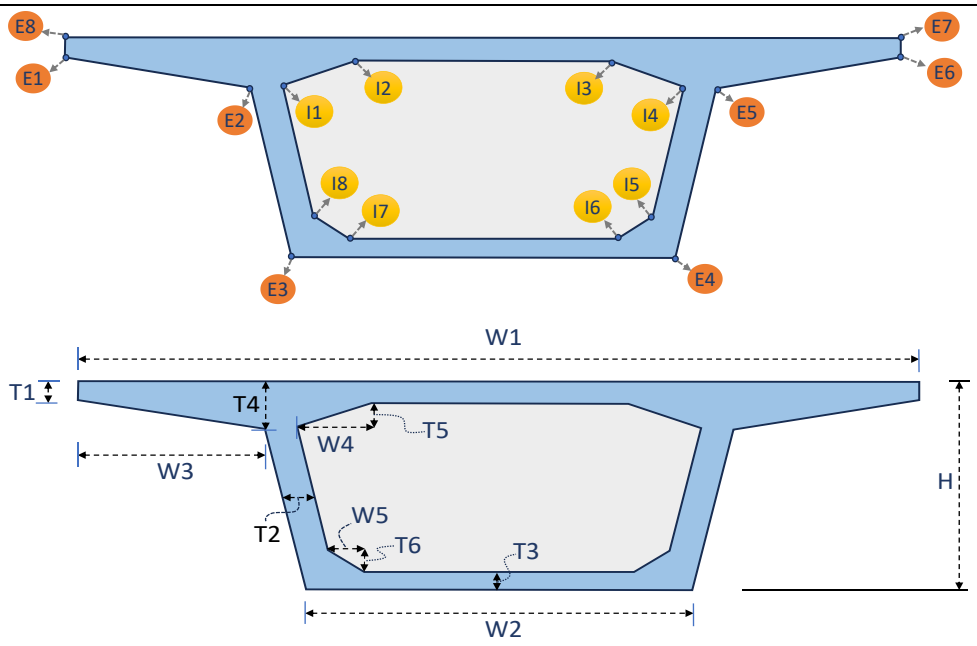

Points	X	Y	Points	X	Y
E1	0	H-T1	I1	W3+T2	H-T4
E2	W3	H-T4	I2	W3+T2+W4	H-T4+T5
E3	(W1-W2)/2	0	I3	W1-W3-T2-W4	H-T4+T5
E4	(W1+W2)/2	0	I4	W1+W3-T2	H-T4
E5	W1-W3	H-T4	I5	W1-[(W1-W2)/2-(T3+T6)*tan(alpha)+T2]	T3+T6
E6	W1	H-T1	I6	X(I5)-W5	T3
E7	W1	H	I7	W1-X(I5)+W5	T3
E8	0	H	I8	W1-X(I5)	T3+T6

where: *alpha = actan([(W1-W2)/2-W3]/(H-T4)]*

Comparison of envelope curves for displacement and acceleration derived using the Finite Element Method (FEM) with the proposed model

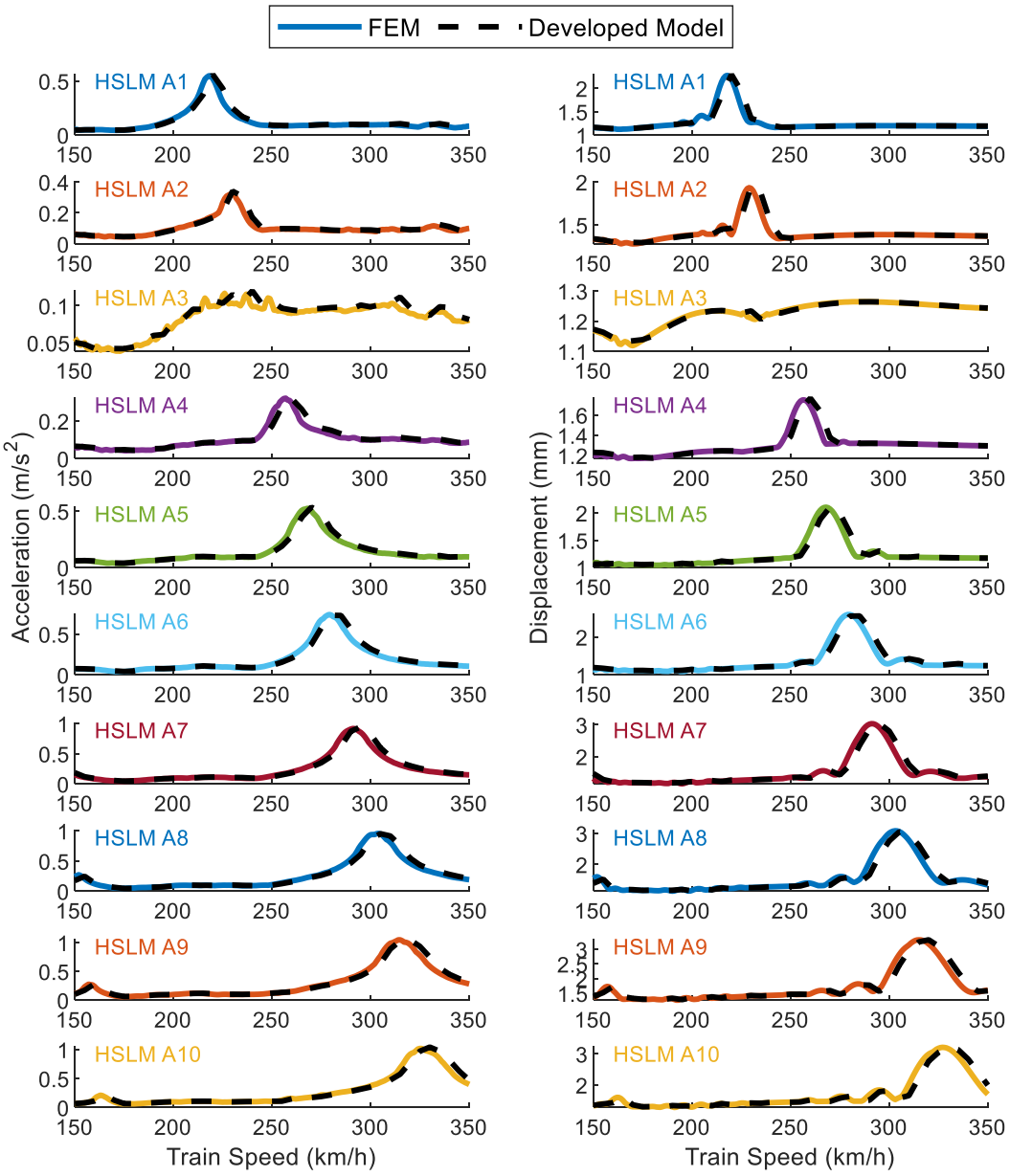

Figure 21. Antoing Bridge

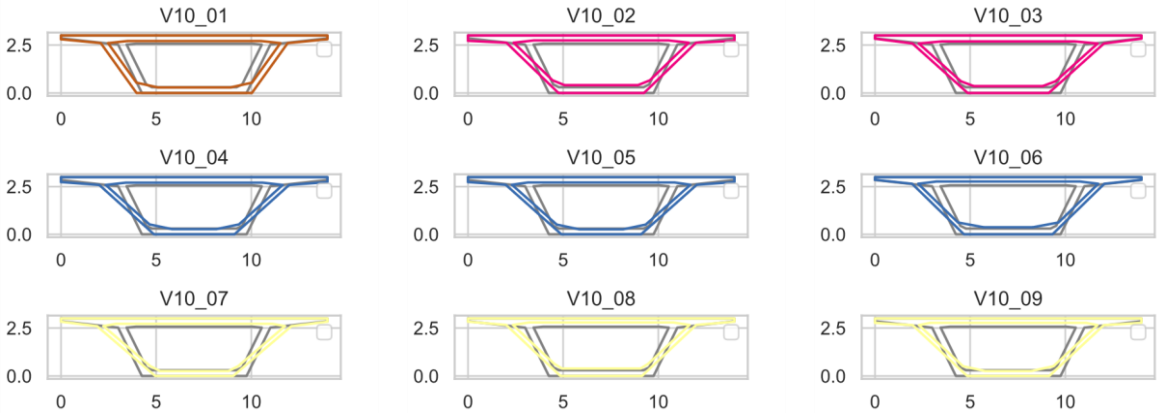

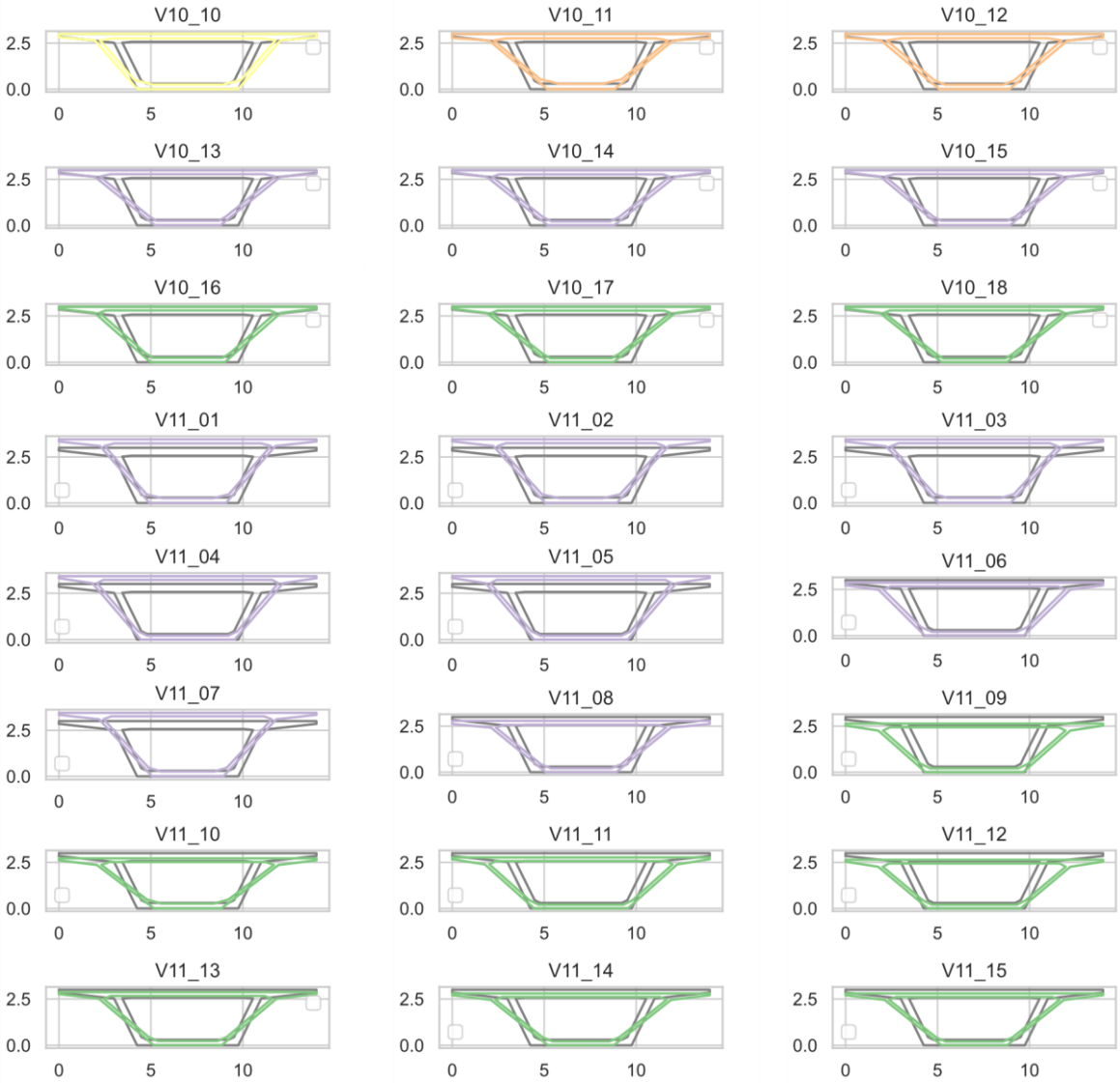

729 **Figure 22. Geometry Comparison of Selected Solutions Relative to the Reference design, Coloured by Mass per Unit**
730 **Length**

731

732

References

[1] H. Xia, N. Zhang, Dynamic analysis of railway bridge under high-speed trains, Comput. Struct. 83 (2005) 1891–1901. https://doi.org/10.1016/j.compstruc.2005.02.014.

[2] B. Yan, G.-L. Dai, N. Hu, Recent development of design and construction of short span high-speed railway bridges in China, Eng. Struct. 100 (2015) 707–717. https://doi.org/10.1016/j.engstruct.2015.06.050.

[3] X. He, T. Wu, Y. Zou, Y.F. Chen, H. Guo, Z. Yu, Recent developments of high-speed railway bridges in China, Struct. Infrastruct. Eng. 13 (2017) 1584–1595. https://doi.org/10.1080/15732479.2017.1304429.

[4] Y. Yang, J. Yau, LC. Hsu, Vibration of simple beams due to trains moving at high speeds, Eng Struct 19 (1997) 936.

[5] M. Fawad, M. Salamak, Q. Chen, M. Uscilowski, K. Koris, M. Jasinski, P. Lazinski, D. Piotrowski, Development of immersive bridge digital twin platform to facilitate bridge damage assessment and asset model updates, Comput. Ind. 164 (2025) 104189. https://doi.org/10.1016/j.compind.2024.104189.

[6] S. Ju, HT. Lin, Resonance characteristics of high-speed trains passing simply supported bridges, J Sound Vib 267 (2003) 1127.

[7] J. Hansen, K. Hanna, M.K. Tadros, Simplified transverse post-tensioning construction and maintenance of adjacent box girders, PCI J. 57 (2012) 64–79. https://doi.org/10.15554/pcij.03012012.64.79.

[8] A. EI-Remaily, M.K. Tadros, T. Yamane, G. Krause, Transverse Design of Adjacent Precast Prestressed Concrete Box Girder Bridges, PCI J. 41 (1996) 96–113. https://doi.org/10.15554/pcij.07011996.96.113.

[9] L.-H. Tran, T.-M. Duong, B. Claudet, K. Le-Nguyen, A. Nordborg, F. Schmidt, Comparative analysis of beam models for vertical rail vibrations under dynamic forces, Eur. J. Mech. - ASolids 110 (2025) 105497. https://doi.org/10.1016/j.euromechsol.2024.105497.

[10] J. Lall, S. Alampalli, E.F. DiCocco, Performance of Full-Depth Shear Keys in Adjacent Prestressed Box Beam Bridges, PCI J. 43 (1998) 72–79. https://doi.org/10.15554/pcij.03011998.72.79.

[11] X. Zhang, W. Zhai, Z. Chen, Characteristic and mechanism of structural acoustic radiation for box girder bridge in urban rail transit, Sci Total Env. 627 (2018) 1303.

[12] J. Su, X. Ma, B. Chen, K. Sennah, Full-scale bending test and parametric study on a 30-m span prestressed ultra-high performance concrete box girder, Adv. Struct. Eng. 23 (2020) 1276–1289. https://doi.org/10.1177/1369433219894244.

[13] A. Fam, H. Honickman, Built-up hybrid composite box girders fabricated and tested in flexure, Eng. Struct. 32 (2010) 1028–1037. https://doi.org/10.1016/j.engstruct.2009.12.029.

[14] G. Dai, M. Su, Y.F. Chen, Design and Construction of Simple Beam Bridges for High-Speed Rails in China: Standardization and Industrialization, Balt. J. Road Bridge Eng. 11 (2016) 274–282. https://doi.org/10.3846/bjrbe.2016.32.

[15] Y. Yang, JD. Yau, Resonance of high-speed trains moving over a series of simple or continuous beams with non-ballasted tracks, Eng Struct 143 (2017) 295.

[16] H. Xia, G. De Roeck, N. Zhang, Experimental analysis of a high-speed railway bridge under Thalys trains, J Sound Vib 268 (2003) 103.

[17] Y. Cao, H. Xia, Z. Li, A semi-analytical/FEM model for predicting ground vibrations induced by high-speed train through continuous girder bridge, J Mech Sci Technol 26 (2012) 2485.

[18] N. Khoshamadi, S. Banihashemi, M. Poshdar, H. Abbasianjahromi, A. Tabadkani, A. Hajirasouli, Parametric and generative mechanisms for infrastructure projects, Autom. Constr. 154 (2023) 104968. https://doi.org/10.1016/j.autcon.2023.104968.

[19] N.K. Kedia, R. Wangtawesap, C. Ngamkhanong, Dynamics responses of railway bridges influenced by flooded ballasted tracks subjected to high-speed trains, Transp. Eng. 20 (2025) 100334. https://doi.org/10.1016/j.treng.2025.100334.

[20] M. Martínez-Rodrigo, J. Lavado, P. Museros, Dynamic performance of existing high-speed railway bridges under resonant conditions retrofitted with fluid viscous dampers, Eng Struct 32 (2010) 808.

[21] G. Gu, Resonance in long-span railway bridges carrying TGV trains, Comput Struct 152 (2015) 185.

[22] José M. Goicolea, Resonant effects in short span high speed railway bridges: modelling and design issues, (2011).

[23] L. Diachenko, A. Benin, A. Diachenko, Research of interaction of the "train – bridge" system with bridge deck resonant vibrations, MATEC Web Conf. 239 (2018) 05002. https://doi.org/10.1051/matecconf/201823905002.

[24] G. Bianchi, C. Fanelli, F. Freddi, F. Giuliani, A. La Placa, Systematic review railway infrastructure monitoring: From classic techniques to predictive maintenance, Adv. Mech. Eng. 17 (2025) 16878132241285631. https://doi.org/10.1177/16878132241285631.

[25] T. Arvidsson, R. Karoumi, Train–bridge interaction – a review and discussion of key model parameters, Int J Rail Transp 2 (2014) 147.

[26] T. Arvidsson, R. Karoumi, Train–bridge interaction–a review and discussion of key model parameters, Int. J. Rail Transp. 2 (2014) 147–186.

[27] T. Arvidsson, R. Karoumi, Train–bridge interaction – a review and discussion of key model parameters, Int. J. Rail Transp. 2 (2014) 147–186. https://doi.org/10.1080/23248378.2014.897790.

[28] British Standards Institution, Eurocode 1: Actions on structures - Part 2: Traffic loads on bridges (BS EN 1991-2:2003), (2003).

[29] C. Blanquart, M. Koning, The local economic impacts of high-speed railways: theories and facts, Eur. Transp. Res. Rev. 9 (2017) 1–14. https://doi.org/10.1007/s12544-017-0233-0.

[30] M. Reiterer, A. Firus, A. Vorwagner, G. Lombaert, J. Schneider, A.M. Kohl, Railway bridge dynamics: development of a new high-speed train load model for dynamic analyses of train crossing, in: IABSE Congr. Ghent 2021, 2021: pp. 1633–1642. https://doi.org/10.2749/ghent.2021.1633.

[31] K. Le Nguyen, Application of XGBoost Model for Predicting the Dynamic Response of High-Speed Railway Bridges, in: C. Ha-Minh, A.M. Tang, T.Q. Bui, X.H. Vu, D.V.K. Huynh (Eds.), CIGOS 2021 Emerg. Technol. Appl. Green Infrastruct., Springer, Singapore, 2022: pp. 1765–1773. https://doi.org/10.1007/978-981-16-7160-9_178.

[32] R. Allahvirdizadeh, A. Andersson, R. Karoumi, Probabilistic Dynamic Design Curves Optimized for High-Speed Reinforced Concrete Railway Bridges Using First-Order Reliability Method, Int. J. Struct. Stab. Dyn. (2024) 2540012. https://doi.org/10.1142/S0219455425400127.

[33] J.-R. Cho, K. Jung, K. Cho, J.-W. Kwark, Y.J. Kim, B.-S. Kim, Determination of the optimal span length for a railway bridge crossed by various types of high-speed trains, Proc. Inst. Mech. Eng. Part F J. Rail Rapid Transit 230 (2016) 531–543. https://doi.org/10.1177/0954409714549083.

[34] T. Cho, M.-K. Song, D.H. Lee, Reliability analysis for the uncertainties in vehicle and high-speed railway bridge system based on an improved response surface method for nonlinear limit states, Nonlinear Dyn. 59 (2010) 1–17. https://doi.org/10.1007/s11071-009-9521-0.

[35] W. Zhai, Z. Han, Z. Chen, L. Ling, S. Zhu, Train–track–bridge dynamic interaction: a state-of-the-art review, Veh. Syst. Dyn. 57 (2019) 984–1027.

[36] R. Allahvirdizadeh, A. Andersson, R. Karoumi, Probabilistic Dynamic Design Curves Optimized for High-Speed Reinforced Concrete Railway Bridges Using First-Order Reliability Method, Int. J. Struct. Stab. Dyn. (2024) 2540012. https://doi.org/10.1142/S0219455425400127.

[37] R. Allahvirdizadeh, A. Andersson, R. Karoumi, Improved dynamic design method of ballasted high-speed railway bridges using surrogate-assisted reliability-based design optimization of dependent variables, Reliab. Eng. Syst. Saf. 238 (2023) 109406. https://doi.org/10.1016/j.ress.2023.109406.

[38] S. Wong, C. Zheng, X. Su, Y. Tang, Construction contract risk identification based on knowledge-augmented language models, Comput. Ind. 157–158 (2024) 104082. https://doi.org/10.1016/j.compind.2024.104082.

[39] I. Dikmen, G. Eken, H. Erol, M.T. Birgonul, Automated construction contract analysis for risk and responsibility assessment using natural language processing and machine learning, Comput. Ind. 166 (2025) 104251. https://doi.org/10.1016/j.compind.2025.104251.

[40] D.M. Onchis, G.-R. Gillich, E. Hogea, C. Tufisi, Neuro-symbolic model for cantilever beams damage detection, Comput. Ind. 151 (2023) 103991. https://doi.org/10.1016/j.compind.2023.103991.

[41] L.-N. Khuong, N. Van Dang, KD-Railway 1.0 – A structural dynamics software for high-speed rail bridge based on open source Cast3m platform, J. Sci. Transp. Technol. (2022).

[42] E. Le Fichoux, Présentation Et Utilisation De Cast3m, (2011). http://www-cast3m.cea.fr/.

[43] ERRI Specialists' Committee D214, Rail Bridges for Speeds > 200km/h, Final Report: Part A Synthesis of the Results of D214 Research, (1999).

[44] L. Frýba, Dynamics of Railway Bridges, T. Telford, 1996.

[45] Y. Yang, CW. Lin, Vehicle-bridge interaction dynamics and potential applications, J Sound Vib 284 (2005) 205.

[46] M. Majka, M. Hartnett, Dynamic response of bridges to moving trains: A study on effects of random track irregularities and bridge skewness, Comput. Struct. 87 (2009) 1233–1252. https://doi.org/10.1016/j.compstruc.2008.12.004.

[47] A. Doménech, P. Museros, M.D. Martínez-Rodrigo, Influence of the vehicle model on the prediction of the maximum bending response of simply-supported bridges under high-speed railway traffic, Eng. Struct. 72 (2014) 123–139. https://doi.org/10.1016/j.engstruct.2014.04.037.

[48] P. Salcher, C. Adam, A. Kuisle, A Stochastic View on the Effect of Random Rail Irregularities on Railway Bridge Vibrations, Struct. Infrastruct. Eng. 15 (2019) 1649–1664. https://doi.org/10.1080/15732479.2019.1640748.

[49] A. Pere, Dynamic Analysis of High Speed 2 Rail: HS2 Project, (n.d.). https://www.midasbridge.com/en/blog/casestudy/dynamic-analysis-of-high-speed-rail-insights-from-the-hs2-project (accessed December 10, 2023).

[50] K. Deb, S. Agrawal, A. Pratap, T. Meyarivan, A Fast Elitist Non-dominated Sorting Genetic Algorithm for Multi-objective Optimization: NSGA-II, in: M. Schoenauer, K. Deb, G. Rudolph, X. Yao, E. Lutton, J.J. Merelo, H.-P. Schwefel (Eds.), Parallel Probl. Solving Nat. PPSN VI, Springer Berlin Heidelberg, Berlin, Heidelberg, 2000: pp. 849–858. https://doi.org/10.1007/3-540-45356-3_83.